



OPEN

Optimal control analysis for the Nipah infection with constant and time-varying vaccination and treatment under real data application

Muhammad Younas Khan¹, Saif Ullah^{1,4}, Muhammad Farooq¹, Basem Al Alwan² & Abdul Baseer Saqib³✉

In the last two decades, Nipah virus (NiV) has emerged as a significant paramyxovirus transmitted by bats, causing severe respiratory illness and encephalitis in humans. NiV has been included in the World Health Organization's Blueprint list of priority pathogens due its potential for human-to-human transmission and zoonotic characteristics. In this paper, a mathematical model is formulated to analyze the dynamics and optimal control of NiV. In formulation of the model we consider two modes of transmission: human-to-human and food-borne. Further, the impact of contact with an infected corpse as a potential route for virus transmission is also consider in the model. The analysis identifies the model with constant controls has three equilibrium states: the NiV-free equilibrium, the infected flying foxes-free equilibrium, and the NiV-endemic equilibrium state. Furthermore, a theoretical analysis is conducted to presents the stability of the model equilibria. The model fitting to the reported cases in Bangladesh from 2001 to 2015, and the estimation of parameters are performed using the standard least squares technique. Sensitivity analysis of the model-embedded parameters is provided to set the optimal time-dependent controls for the disease eradication. The necessary optimality conditions are derived using Pontryagin's maximum principle. Finally, numerical simulation is performed to determine the most effective strategy for disease eradication and to confirm the theoretical results.

Keywords NiV outbreak, Constant and time-varying controls, Sensitivity analysis, Pontryagin's maximum principle, Simulation

NiV is a zoonotic viral infection that belongs to the Paramyxoviridae family. It can be transmitted through contaminated food and directly between humans¹. The virus can cause various respiratory infections in both animals and humans¹. The Pteropus genus, specifically the Pteropodidae family of flying foxes are the natural reservoir for the NiV^{1,2}. More than 50 different species of Pteropus bats are found in the south and southeast Asian regions³. NiV can be transmitted to humans through various transmission routes, either directly from flying foxes or indirectly from animals that have been infected by them. Another mean of viral transmission is through unsafe contact with the dead body of an infected person prior to their funeral or burial¹⁻⁵. A person infected with Nipah experience symptoms like headache, fever, and tiredness during the first 2 weeks after virus exposure. These symptoms in some cases lead to a coma within 2 days^{6,7}. There is currently no vaccine available to prevent the NiV, so the best way to contain its spread is by educating people and raising awareness³.

NiV was first discovered during an outbreak of encephalitis and respiratory diseases in a Malaysian village called Sungai Nipah. From September 1998 till April 1999, there were 265 infected cases resulting in 105 mortalities. It was found that pigs were the carriers of the virus, and they infected pig farmers, leading to the outbreak^{5,8}.

¹Department of Mathematics, University of Peshawar, Peshawar, KP 25000, Pakistan. ²Chemical Engineering Department, College of Engineering, King Khalid University, Abha 62521, Saudi Arabia. ³Faculty of Education, Department of Mathematics, Nangarhar University, Nangarhar, Afghanistan. ⁴Department of Mathematics, Faculty of Science and Technology, Universitas Airlangga, Surabaya 60115, Indonesia. ✉email: ab_saqib@nu.edu.af

In 1998, Malaysia experienced a severe Nipah epidemic, and from 2001 to 2012, occasional outbreaks of the disease occurred in Bangladesh. Nipah also re-emerged periodically in India near the Bangladesh border and West Bengal. Furthermore, in 2018, a Nipah outbreak occurred in Kerala, a southern region of India, even though it was 2,800 kilometers away from the Bangladesh border and was not in the usual outbreak season.

In South-East Asian nations, palm sap obtained from date palms is widely consumed³. The crop is typically collected in the colder months, especially in the rural areas of Bangladesh⁹. Flying foxes contaminate date palm sap with excretions like saliva and urine when feeding. In Bangladesh, it has been observed that Nipah disease can be transmitted to humans through the consumption of contaminated fruits or fruit products that might have been contaminated by flying foxes¹⁰. The transmission from human-to-human was identified during the NiV outbreak in Bangladesh reported 2004¹¹. The infection was transfer to the individuals who had direct exposure to the body fluids of individuals infected with NiV, or through the use of contaminated materials such as towels, bedsheets, etc. This included medical practitioners, family caregivers, and hospital visitors¹².

Mathematical modeling is a useful approach for analyzing and simulating real-life problems, including epidemic outbreaks^{13–16}. These models are usually constructed via system of ordinary or partial differential equations and are helpful to set an effective control interventions for disease minimization^{17–19}. Various compartmental models can be found in the existing literature that explain the transmission dynamics of the NiV incidence in different countries and suggest possible effective measures to eradicate it. In²⁰, a transmission modeling approach was utilized to determine the optimal preventive measures for the control of NiV in the population of Bangladesh. Beside this many papers have been published to explore the dynamical aspects of the infection transmission and possible controlling strategies. Mondal et al.²¹ examined a compartmental model to explore how prevention strategies can minimize the incidence of disease. Shah et al.²² proposed a SEI-type mathematical model considering multiple transmission modes, including among humans transmission through contact with deceased NiV patients. Nita et al.²³ proposed a new epidemic model that takes into account the connection between bats and humans, incorporating various control strategies such as hospitalizations, self-prevention, spraying pesticides, and burying flying foxes. Agarwal and Singh²⁴ proposed a transmission model that accounts for both human and flying fox populations, which has significant implications for understanding and preventing the transmission of zoonotic diseases. A recent analysis focusing on the mitigation of NiV via a Caputo fractional optimal control problem was presented in²⁵. The global dynamics and various transmission aspects of NiV were studied in^{26–28}.

This research emphasizes on presenting a comparative analysis of time-dependent and constant controlling strategies for the mitigation of NiV with vaccination and treatment using optimal control theory. To do so, we develop a compartmental model that considers various factors, building on previous research. A sensitivity analysis will be performed to find out the influential parameters embedded in the model. Optimal control theory will then be applied by introducing six control variables to mitigate the incidence of the infection in the community. The paper is divided into seven sections. In the next section the development procedure of the model with brief description of the parameters will be presented. Section “[Qualitative analysis of NiV model](#)” covers qualitative analysis, calculation of reproduction number, and performing stabilities. Section “[Application to the outbreak reported in Bangladesh during 2001–2015](#)” discusses data fitting. In the section “[Sensitivity of the threshold parameters](#)” a normalized sensitivity analysis of the model parameters is conducted. Section “[Formulation of the optimal control NiV model](#)” focuses on optimal control analysis, numerical simulations, and graphical results. The final concluding remarks are shown in section “[Conclusion](#)”.

Model formulation with constant control measures

This section presents a brief procedure used to develop the proposed model exploring the dynamics of NiV. The transmission of the virus can occur via two modes: food-borne transmission, which happens when contaminated food is consumed, and direct transmission among humans from both infected and deceased individuals. The resulting NiV epidemic model consists of nine equations that capture the dynamical aspects of various population groups. The representation of virus shedding by flying foxes at any given time is denoted by the variable $V(t)$. The flying fox population is divided into susceptible (S_f) and infected (I_f) groups. Flying foxes carrying the virus can infect humans. The human population is further divided into six sub-groups: susceptible humans, represented as S_h , vaccinated humans, represented as V_h , infected humans, represented as I_h , treated humans, represented as T_h , recovered humans, represented as R_h , and deceased human bodies, represented as D_h . The total flying fox population is represented as $N_f = S_f + I_f$, and the total human population is represented as $N_h = S_h + V_h + I_h + T_h + R_h$. The dynamics in each class can be described as follows.

Dynamics of flying foxes

The recruitment rate of S_f is denoted as Λ_f , while their natural death rate is represented by d_f . When S_f interacts with the Nipah virus, they have a chance of becoming infected at a rate of β_1 , subsequently moving to the infectious class. The infectious flying foxes pass away at a rate of d_f . Thus,

$$S'_f(t) = \Lambda_f - \frac{\beta_1 V}{N_f} S_f - d_f S_f, \quad (1)$$

and

$$I'_f(t) = \frac{\beta_1 V}{N_f} S_f - d_f I_f. \quad (2)$$

Dynamics of the nipah viral concentration

To better understand the transmission dynamics of viruses among flying foxes we construct the following equation

$$V'(t) = pI_f - \theta V, \quad (3)$$

where p and θ are the virus shedding and decay rates respectively.

Dynamics of human population

The transmission of the Nipah virus occurs in three ways: through contaminated food (at a rate of β_2), through direct contact between infected and susceptible individuals (at a rate of β_3), and through touching the bodies of people who have been infected and have died (at a rate of β_4 , with a fraction of κ indicating those dead bodies not properly handled leading to the spread of NiV). The force of infection can be calculated by taking into account all three transmission rates. Thus we have:

$$\lambda_h = \frac{\beta_2 V + \beta_3 I_h + \beta_4 \kappa D_h}{N_h}. \quad (4)$$

The rate at which the human population is recruited is denoted by Λ_h . The susceptible population increases at a rate of γ , which represents waning of immunity. Furthermore, vaccinated individuals rejoin the susceptible class at a rate of ζ due to vaccine waning immunity. Conversely, the susceptible population decreases due to three factors: interaction with contaminated food and infected humans, represented by the force of infection λ_h ; vaccination at the rate ξ ; and the natural death rate d_h . Thus, we have:

$$S'_h(t) = \Lambda_h - \frac{(\beta_2 V + \beta_3 I_h + \beta_4 \kappa D_h)}{N_h} S_h - (d_h + \xi) S_h + \gamma R_h + \zeta V_h. \quad (5)$$

The vaccinated human population increases as susceptible individuals join it at a rate of ξ . The population is reduced by natural death rates of d_h , and due vaccine waning immunity at the rate ζ .

$$V'_h(t) = \xi S_h - (\zeta + d_h) V_h. \quad (6)$$

When susceptible individuals are infected with a disease, the number of infected individuals increases. This is due to the force of infection, denoted by λ_h . However, the population of infected individuals decreases due to various factors such as recovery rate α_1 , treatment rate ρ , disease-related mortality d_1 , and natural mortality rate d_h .

$$I'_h(t) = \frac{(\beta_2 V + \beta_3 I_h + \beta_4 \kappa D_h)}{N_h} S_h - (\rho + \alpha_1 + d_1 + d_h) I_h. \quad (7)$$

The infected people join treatment class at the flow rate ρ . This class is reduced after getting recovery at a rate α_2 and natural mortality d_h .

$$T'_h(t) = \rho I_h - (\alpha_2 + d_h) T_h. \quad (8)$$

The recovered individuals increase through the induction of the infected and treated individuals at a steady influx rate of α_1 and α_2 , respectively. Additionally, a decrease in the recovered population occurs due to natural death and loss of immunity, indicated by the rates d_h and γ , respectively.

$$R'_h(t) = \alpha_1 I_h + \alpha_2 T_h - (\gamma + d_h) R_h. \quad (9)$$

The individuals who die due to NiV infection are added to the deceased class at a rate of d_1 . The deceased individuals are buried at a rate of ν .

$$D'_h(t) = d_1 I_h - \nu D_h. \quad (10)$$

By combining the aforementioned differential equations, the dynamics of Nipah virus can be modeled by a system of nonlinear differential equations as follows:

$$\begin{cases} S'_f(t) = \Lambda_f - \frac{\beta_1 V}{N_f} S_f - d_f S_f, \\ I'_f(t) = \frac{\beta_1 V}{N_f} S_f - d_f I_f, \\ V'(t) = pI_f - \theta V, \\ S'_h(t) = \Lambda_h - \frac{(\beta_2 V + \beta_3 I_h + \beta_4 \kappa D_h)}{N_h} S_h - (d_h + \xi) S_h + \gamma R_h + \zeta V_h, \\ V'_h(t) = \xi S_h - (\zeta + d_h) V_h, \\ I'_h(t) = \frac{(\beta_2 V + \beta_3 I_h + \beta_4 \kappa D_h)}{N_h} S_h - (\rho + \alpha_1 + d_1 + d_h) I_h, \\ T'_h(t) = \rho I_h - (\alpha_2 + d_h) T_h, \\ R'_h(t) = \alpha_1 I_h + \alpha_2 T_h - (\gamma + d_h) R_h, \\ D'_h(t) = d_1 I_h - \nu D_h, \end{cases} \quad (11)$$

where the initial conditions (ICs) are given by

$$\begin{cases} S_f(0) = S_{f0} \geq 0, I_f(0) = I_{f0} \geq 0, V(0) = V_0 \geq 0, S_h(0) = S_{h0} \geq 0, V_h(0) = V_{h0} \geq 0, \\ I_h(0) = I_{h0} \geq 0, T_h(0) = T_{h0} \geq 0, R_h(0) = R_{h0} \geq 0, D_h(0) = D_{h0} \geq 0. \end{cases} \tag{12}$$

**Qualitative analysis of NiV model
Invariantly positive region**

The region having biological feasibility for the problem (11) is shown in the following set

$$\Theta = \Theta_f \times \Theta_h \subset \mathbb{R}_+^3 \times \mathbb{R}_+^6,$$

where

$$\begin{aligned} \Theta_f &= \left\{ (S_f, I_f, V) \in \mathbb{R}_+^3 : N_f = S_f + I_f = \frac{\Lambda_f}{d_f}, V \leq \frac{p\Lambda_f}{\theta d_f} \right\}, \\ \Theta_h &= \left\{ (S_h, V_h, I_h, T_h, R_h, D_h) \in \mathbb{R}_+^6 : N_h = S_h + V_h + I_h + T_h + R_h \leq \frac{\Lambda_h}{d_h}, D_h \leq \frac{\Lambda_h d_1}{v d_h} \right\}. \end{aligned}$$

Theorem 1 *The model (11) with the ICs defined in (12) has a positive invariant solution in $\Theta = \Theta_f \times \Theta_h$.*

Proof It is easy to demonstrate that entire solutions originating from nonnegative ICs will also remain nonnegative $\forall t > 0$. Furthermore, from the model (11), we proceed as follows

$$\begin{aligned} N_f'(t) &= S_f'(t) + I_f'(t), \\ &= \Lambda_f - d_f N_f, \end{aligned}$$

alternatively,

$$N_f'(t) + d_f N_f = \Lambda_f. \tag{13}$$

Applying the Laplace transformation

$$\begin{aligned} \mathcal{L}[N_f'(t) + d_f N_f] &= \mathcal{L}[\Lambda_f], \\ sY(s) - N_f(0) + d_f Y(s) &= \frac{\Lambda_f}{s}, \\ (s + d_f)Y(s) &= N_{f0} + \frac{\Lambda_f}{s}, \\ Y(s) &= \frac{N_{f0}}{s + d_f} + \frac{\Lambda_f}{s(s + d_f)}. \end{aligned}$$

The inverse Laplace further gives the following form:

$$N_f(t) = \frac{\Lambda_f}{d_f} + \left(N_{f0} - \frac{\Lambda_f}{d_f} \right) e^{-d_f t}.$$

We derive that $N_f(t) \leq \frac{\Lambda_f}{d_f}$, if $N_f(0) \leq \frac{\Lambda_f}{d_f}$, whenever $t \rightarrow \infty$. As a result, for $t > 0$, the NiV model (11) solution with ICs in Θ_f remains in Θ_f . A similar procedure leads to the fact that $V(t) \leq \frac{p\Lambda_f}{\theta d_f}$, $N_h(t) \leq \frac{\Lambda_h}{d_h}$ and $D_h(t) \leq \frac{d_1 \Lambda_h}{v d_h}$ as $t > 0$. Therefore, it is concluded that the region Θ possesses positive invariance property and consequently attracts all solutions of the system. \square

Investigation of equilibria and threshold parameter

The NiV epidemic model attains three equilibrium points. The infection-free equilibrium (IFE) is given as follows:

$$E^0 = \left(S_f^0, I_f^0, V^0, S_h^0, V_h^0, I_h^0, T_h^0, R_h^0, D_h^0 \right) = \left(\frac{\Lambda_f}{d_f}, 0, 0, \frac{\Lambda_h(d_h + \zeta)}{d_h(d_h + \zeta + \xi)}, \frac{\xi \Lambda_h}{d_h(d_h + \zeta + \xi)}, 0, 0, 0, 0 \right). \tag{14}$$

The threshold number, denoted as \mathcal{R}_0 , is derived using the technique presented in²⁹, and given as follows.

$$\mathcal{R}_0 = \max \left\{ \mathcal{R}_f^0, \mathcal{R}_h^0 \right\} = \max \left\{ \mathcal{R}_f^0, \mathcal{R}_{h_1}^0 + \mathcal{R}_{h_2}^0 \right\} = \max \left\{ \frac{p\beta_1}{\theta d_f}, \frac{\beta_3 c_2}{c_3(c_2 + \xi)} + \frac{d_1 \beta_4 \kappa c_2}{v c_3(c_2 + \xi)} \right\}, \tag{15}$$

where, $c_2 = (\zeta + d_h)$ and $c_3 = (\rho + \alpha_1 + d_1 + d_h)$.

Stability of the model

After applying the Jacobian method to the system (11), it is possible to confirm the local stability of IFE.

Theorem 2 For $\mathcal{R}_0 < 1$, the equilibrium is locally asymptotically stable (LAS), while it is unstable otherwise.

Proof At the infection-free equilibrium, the LAS can be examined by analyzing the Jacobian matrix of system (11). The corresponding Jacobian matrix is evaluated as follows:

$$J_9 = \begin{pmatrix} -\theta & 0 & p & 0 & 0 & 0 & 0 & 0 & 0 \\ -\beta_1 & -d_f & 0 & 0 & 0 & 0 & 0 & 0 & 0 \\ \beta_1 & 0 & -d_f & 0 & 0 & 0 & 0 & 0 & 0 \\ -\frac{\beta_2 c_2}{c_2 + \xi} & 0 & 0 & -c_1 & \zeta & -\frac{\beta_3 c_2}{c_2 + \xi} & 0 & \gamma & -\frac{\beta_4 c_2 \kappa}{c_2 + \xi} \\ 0 & 0 & 0 & \xi & -c_2 & 0 & 0 & 0 & 0 \\ \frac{\beta_2 c_2}{c_2 + \xi} & 0 & 0 & 0 & 0 & \frac{\beta_3 c_2}{c_2 + \xi} - c_3 & 0 & 0 & \frac{\beta_4 c_2 \kappa}{c_2 + \xi} \\ 0 & 0 & 0 & 0 & 0 & \rho & -c_4 & 0 & 0 \\ 0 & 0 & 0 & 0 & 0 & \alpha_1 & \alpha_2 & -c_5 & 0 \\ 0 & 0 & 0 & 0 & 0 & d_1 & 0 & 0 & -\nu \end{pmatrix}.$$

The eigenvalue $\lambda_1 = -d_f$ is negative, so we have

$$J_8 = \begin{pmatrix} -\theta & p & 0 & 0 & 0 & 0 & 0 & 0 \\ \beta_1 & -d_f & 0 & 0 & 0 & 0 & 0 & 0 \\ -\frac{\beta_2 c_2}{c_2 + \xi} & 0 & -c_1 & \zeta & -\frac{\beta_3 c_2}{c_2 + \xi} & 0 & \gamma & -\frac{\beta_4 c_2 \kappa}{c_2 + \xi} \\ 0 & 0 & \xi & -c_2 & 0 & 0 & 0 & 0 \\ \frac{\beta_2 c_2}{c_2 + \xi} & 0 & 0 & 0 & \frac{\beta_3 c_2}{c_2 + \xi} - c_3 & 0 & 0 & \frac{\beta_4 c_2 \kappa}{c_2 + \xi} \\ 0 & 0 & 0 & 0 & \rho & -c_4 & 0 & 0 \\ 0 & 0 & 0 & 0 & \alpha_1 & \alpha_2 & -c_5 & 0 \\ 0 & 0 & 0 & 0 & d_1 & 0 & 0 & -\nu \end{pmatrix}.$$

Further, by row operation, we have

$$J_8 = \begin{pmatrix} -\theta & p & 0 & 0 & 0 & 0 & 0 & 0 \\ 0 & a_{22} & 0 & 0 & 0 & 0 & 0 & 0 \\ 0 & 0 & -c_1 & \zeta & -\beta_3 & 0 & \gamma & -\beta_4 \kappa \\ 0 & 0 & 0 & b_{44} & b_{45} & 0 & b_{47} & b_{48} \\ 0 & 0 & 0 & 0 & \beta_3 - c_3 & 0 & 0 & \beta_4 \kappa \\ 0 & 0 & 0 & 0 & \rho & -c_4 & 0 & 0 \\ 0 & 0 & 0 & 0 & c_{75} & 0 & -c_5 & 0 \\ 0 & 0 & 0 & 0 & d_1 & 0 & 0 & -\nu \end{pmatrix},$$

where $a_{22} = \frac{\beta_1 p - d_f \theta}{\theta}$, $b_{44} = \frac{\xi \zeta - c_1 c_2}{c_1}$, $b_{45} = \frac{-\beta_3 \xi}{c_1}$, $b_{47} = \frac{\gamma \xi}{c_1}$, $b_{48} = \frac{-\beta_4 \xi \kappa}{c_1}$, $c_{75} = \frac{\alpha_1 c_4 + \alpha_2 \rho}{c_4}$. This implies that the eigenvalues i.e., $\lambda_2 = -\theta$, $\lambda_3 = -c_1$, $\lambda_4 = -c_4$ are also negatives.

To further evaluate, we will take the sub-matrix

$$J_5 = \begin{pmatrix} a_{22} & 0 & 0 & 0 & 0 \\ 0 & b_{44} & b_{45} & b_{47} & b_{48} \\ 0 & 0 & \beta_3 - c_3 & 0 & \beta_4 \kappa \\ 0 & 0 & c_{75} & -c_5 & 0 \\ 0 & 0 & d_1 & 0 & -\nu \end{pmatrix}.$$

The eigenvalues that are included in the Jacobian matrix J_5 , can be obtained by finding the roots of its characteristic equation. These eigenvalues correspond to the remaining eigenvalues of J_9 .

$$\lambda_h^{*5} + l_1 \lambda_h^{*4} + l_2 \lambda_h^{*3} + l_3 \lambda_h^{*2} + l_4 \lambda_h^{*} + l_5 = 0, \tag{16}$$

where,

$$\begin{aligned}
 l_1 &= c_3(1 - \mathcal{R}_{h1}^0) + c_5 + v + d_f(1 - \mathcal{R}_f^0) + \frac{c_1 c_2 - \xi \zeta}{c_1}, \\
 l_2 &= c_3 v(1 - \mathcal{R}_h^0) + c_5(c_3(1 - \mathcal{R}_{h1}^0) + v) + \left\{ d_f(1 - \mathcal{R}_f^0) + \frac{c_1 c_2 - \xi \zeta}{c_1} \right\} \{c_3(1 - \mathcal{R}_{h1}^0) + c_5 + v\} \\
 &\quad + d_f(1 - \mathcal{R}_f^0) \left\{ \frac{c_1 c_2 - \xi \zeta}{c_1} \right\}, \\
 l_3 &= \left\{ d_f(1 - \mathcal{R}_f^0) + \frac{c_1 c_2 - \xi \zeta}{c_1} \right\} \{c_5(c_3(1 - \mathcal{R}_{h1}^0) + v) + c_3 v(1 - \mathcal{R}_h^0)\} \\
 &\quad + c_3 c_5 v(1 - \mathcal{R}_h^0) + \left\{ \frac{c_1 c_2 - \xi \zeta}{c_1} \right\} \{c_3(1 - \mathcal{R}_{h1}^0) + c_5 + v\} \{d_f(1 - \mathcal{R}_f^0)\}, \\
 l_4 &= c_3 c_5 v \left\{ d_f(1 - \mathcal{R}_f^0) + \frac{c_1 c_2 - \xi \zeta}{c_1} \right\} \{c_3(1 - \mathcal{R}_{h1}^0)\} + \{d_f(1 - \mathcal{R}_f^0)\} \left\{ \frac{c_1 c_2 - \xi \zeta}{c_1} \right\} \{c_5 c_3(1 - \mathcal{R}_{h1}^0) \\
 &\quad + v(c_3(1 - \mathcal{R}_h^0) + c_5)\}, \\
 l_5 &= c_3 c_5 v \{d_f(1 - \mathcal{R}_f^0)\} \left\{ \frac{c_1 c_2 - \xi \zeta}{c_1} \right\} \{(1 - \mathcal{R}_h^0)\}.
 \end{aligned}$$

Clearly, all $l_i, i=1, \dots, 5$, are positive if \mathcal{R}_h^0 . Hence the equilibrium is LAS if $\mathcal{R}_h^0 < 1$. □

Infected flying foxes-free equilibrium state

Theorem 3 *In the NiV model (11), if $\mathcal{R}_0 > 1$, \exists a unique infected flying-foxes free equilibrium (IFFE).*

Proof By solving Eq. (11) simultaneously for virus and human compartments, we obtain an expression for $S_f = \frac{\Lambda_f}{d_f}, I_f = 0$, and $V = 0$, the in terms of the IFFE point we have the following set

$$E_h^* = \left(\frac{\Lambda_f}{d_f}, 0, 0, S_h^*, V_h^*, I_h^*, T_h^*, R_h^*, D_h^* \right), \tag{17}$$

such that

$$\begin{cases}
 S_h^* = \frac{c_2 c_3 c_4 c_5 \Lambda_h}{c_3 c_4 c_5 (c_1 c_2 - \xi \zeta) + c_2 \lambda_h (c_3 c_4 c_5 - \gamma (\alpha_1 c_4 + \alpha_2 \rho))}, \\
 V_h^* = \frac{\xi}{c_2} S_h^*, \\
 I_h^* = \frac{1}{c_3} \lambda_h^* S_h^*, \\
 T_h^* = \frac{\rho}{c_3 c_4} \lambda_h^* S_h^*, \\
 R_h^* = \frac{(\alpha_1 c_4 + \alpha_2 \rho)}{c_3 c_4 c_5} \lambda_h^* S_h^*, \\
 D_h^* = \frac{d_1}{v c_3} \lambda_h^* S_h^*,
 \end{cases} \tag{18}$$

where,

$$\lambda_h^* = \frac{\beta_2 V^* + \beta_3 I_h^* + \beta_4 \kappa D_h^*}{N_h^*}. \tag{19}$$

Further, putting (18) in (19), we obtain

$$\varrho_1 \lambda_h^* + \varrho_2 = 0, \tag{20}$$

where the coefficients are

$$\begin{aligned}
 \varrho_1 &= c_3 c_4 c_5 v \Lambda_h (\xi + (1 - \mathcal{R}_h^0)), \\
 \varrho_2 &= c_2 v \Lambda_h (\alpha_2 \rho + \alpha_1 c_4 + c_5 (c_4 + \rho)).
 \end{aligned}$$

Hence, a unique IFFE point exists if $\mathcal{R}_h^0 > 1$. □

NiV-endemic equilibrium

From the NiV epidemic model (11) we obtain

$$E^{**} = \left(S_f^{**}, I_f^{**}, V^{**}, S_h^{**}, V_h^{**}, I_h^{**}, T_h^{**}, R_h^{**}, D_h^{**} \right), \tag{21}$$

such that

$$\begin{cases} S_f^{**} = \frac{\theta \Lambda_f^{**}}{p\beta_1}, \\ I_f^{**} = \frac{\Lambda_f^{**}(p\beta_1 - \theta d_f)}{p\beta_1 d_f}, \\ V^{**} = \frac{\Lambda_f^{**}(p\beta_1 - \theta d_f)}{\beta_1 \theta d_f}, \\ S_h^{**} = \frac{c_2 c_3 c_4 c_5 \Lambda_h}{c_3 c_4 c_5 (c_1 c_2 - \zeta \xi) + c_2 \lambda_h (c_3 c_4 c_5 - \gamma(\alpha_1 c_4 + \alpha_2 \rho))}, \\ V_h^{**} = \frac{\xi}{c_2} S_h^{**}, \\ I_h^{**} = \frac{1}{c_3} \lambda_h^{**} S_h^{**}, \\ T_h^{**} = \frac{\rho}{c_3 c_4} \lambda_h^{**} S_h^{**}, \\ R_h^{**} = \frac{(\alpha_1 c_4 + \alpha_2 \rho)}{c_3 c_4 c_5} \lambda_h^{**} S_h^{**}, \\ D_h^{**} = \frac{d_1}{vc_3} \lambda_h^{**} S_h^{**}. \end{cases} \tag{22}$$

The force of infection term is given as follows

$$\lambda_h^{**} = \frac{\beta_2 V^{**} + \beta_3 I_h^{**} + \beta_4 \kappa D_h^{**}}{N_h^{**}}. \tag{23}$$

Further, putting (22) in (23), we obtain

$$\varpi_1 \lambda_h^{**2} + \varpi_2 \lambda_h^{**} + \varpi_3 = 0, \tag{24}$$

where the coefficients are

$$\begin{aligned} \varpi_2 &= \beta_2 c_3 c_4 c_5 v \Lambda_f (c_1 c_2 - \zeta \xi) (1 - \mathcal{R}_f^0), \\ \varpi_1 &= \beta_2 c_2 v \Lambda_f (1 - \mathcal{R}_f^0) [c_3 c_4 c_5 - \gamma(\alpha_2 \rho + \alpha_1 c_4)] + v c_3 c_4 c_5 \beta_1 \Lambda_h (\xi + c_2) (1 - \mathcal{R}_h^0) \\ \varpi_0 &= \beta_1 c_2 \Lambda_h [(\alpha_1 c_4 + \alpha_2 \rho) + c_5 (c_4 + \rho)]. \end{aligned}$$

Theorem about NVEE is developed as follows.

Theorem 4

- (i) A NVEE point E^{**} exists and will be unique if $\varpi_2 < 0 \iff \mathcal{R}_f \geq 1$.
- (ii) The point E^{**} will be unique if $(\varpi_1 < 0 \wedge \varpi_2 = 0) \vee \varpi_1^2 - 4\varpi_0\varpi_2 = 0$.
- (iii) The model has two NVEE if $\varpi_1 < 0, \varpi_2 > 0$ and the discriminant is positive.
- (iv) An NVEE cannot be found anywhere else.

Proof Following condition (i), there exists a unique NVEE for the said model. □

Global asymptotically stability of the IFE

Theorem 5 For $\mathcal{R}_0 < 1$, then the IFE of (11) is globally asymptotically stable (GAS).

Proof In order to obtain the GAS of (11), a Lyapunov type function say \mathbb{F} is introduced.

$$\mathbb{F} = \mathbb{L}_1 V + \mathbb{L}_2 I_f + \mathbb{L}_3 I_h + \mathbb{L}_4 D_h,$$

Later, we will consider the values of $\mathbb{L}_1, \mathbb{L}_2, \mathbb{L}_3$ and \mathbb{L}_4 . Computing the time derivative of \mathbb{F} yields:

$$\begin{aligned} \mathbb{F}' &= \mathbb{L}_1 V' + \mathbb{L}_2 I_f' + \mathbb{L}_3 I_h' + \mathbb{L}_4 D_h', \\ \mathbb{F}' &= \mathbb{L}_1 (pI_f - \theta V) + \mathbb{L}_2 \left(\frac{\beta_1 V}{N_f} S_f - d_f I_f \right) + \mathbb{L}_3 \left(\frac{(\beta_2 V + \beta_3 I_h + \beta_4 \kappa D_h)}{N_h} S_h - c_3 I_h \right) + \mathbb{L}_4 (d_1 I_h - v D_h), \\ \mathbb{F}' &\leq [-\mathbb{L}_1 \theta + \mathbb{L}_2 \beta_1 + \mathbb{L}_3 \beta_2] V + [\mathbb{L}_1 p - \mathbb{L}_2 d_f] I_f + [\mathbb{L}_3 (\beta_3 - c_3) + \mathbb{L}_4 d_1] I_h + [\mathbb{L}_3 \beta_4 \kappa - \mathbb{L}_4 v] D_h, \end{aligned}$$

Since $S_f \leq N_f$ and $S_h \leq N_h$.

Setting the non-negative values of $\mathbb{L}_1 = \frac{\beta_2 \mathbb{L}_3 + \beta_1 \mathbb{L}_2}{\theta}$, $\mathbb{L}_2 = \frac{p \mathbb{L}_1}{d_f}$, $\mathbb{L}_3 = \frac{c_3 v (c_2 + \xi) - c_2 (\beta_3 v + \beta_4 d_1 \kappa)}{c_3 v - (\beta_3 v + \beta_4 d_1 \kappa)}$, and $\mathbb{L}_4 = \frac{\beta_4 \kappa (c_3 v (c_2 + \xi) - c_2 (\beta_3 v + \beta_4 d_1 \kappa))}{v (c_3 v - (\beta_3 v + \beta_4 d_1 \kappa))}$, we get

$$\begin{aligned} \mathbb{F}' &\leq c_3 (c_2 + \xi) \left(\frac{c_2 (\beta_3 v + \beta_4 d_1 \kappa)}{c_3 v (c_2 + \xi)} - 1 \right) I_h, \\ \mathbb{F}' &\leq c_3 (c_2 + \xi) (\mathcal{R}_h^0 - 1) I_h. \end{aligned}$$

If $\mathcal{R}_f^0 < 1$ and $\mathcal{R}_h^0 < 1$, i.e., if the value of \mathcal{R}_0 is less than one then it can be observed that the derivative of the Lyapunov function \mathbb{F}' , is negative. Therefore, it can be claimed that the IFE of the NiV epidemic model is GAS. □

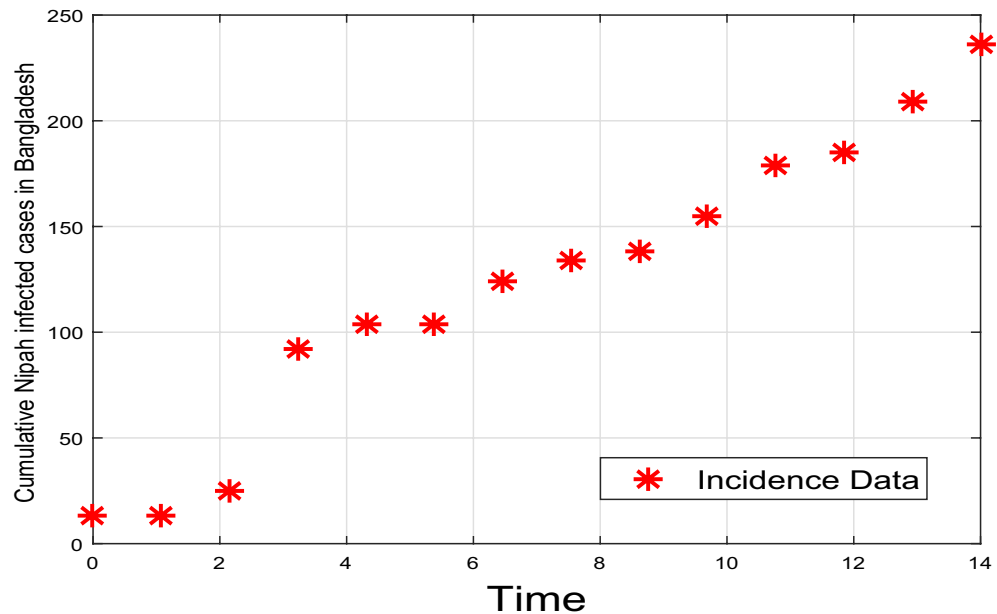


Figure 1. Reported cumulative confirmed cases during from 2001–2015 outbreaks occurred in Bangladesh.

Application to the outbreak reported in Bangladesh during 2001–2015 Epidemiology and outbreak of NiV in Bangladesh

NiV has a considerable influence on public health in Bangladesh. During 2001 to 2015 multiple outbreaks have been reported in Bangladesh. In Bangladesh, NiV outbreaks have occurred primarily in the central and north-western regions of the country, particularly in the districts of Rajshahi, Naogaon, and Faridpur. The disease primarily affects individuals involved in the farming and harvesting of date palm sap, as well as those who come into contact with infected animals, particularly fruit bats (the natural reservoir of the virus), and contaminated food or beverages. NiV infection in Bangladesh typically presents with a range of symptoms, including fever, headache, dizziness, respiratory distress, vomiting, and altered consciousness. In severe cases, it can progress to encephalitis (inflammation of the brain) and lead to coma or death. The disease has a high mortality rate, ranging from 40% to 75% in reported outbreaks. Efforts to control NiV infection in Bangladesh have focused on surveillance and early detection of cases, as well as public health interventions to limit transmission. These interventions include the culling of infected animals, quarantine measures, and public awareness campaigns to educate communities about the risks of the disease and how to prevent transmission. Research efforts have also been directed towards understanding the ecology of the NiV, including its transmission dynamics between bats, intermediate hosts (such as pigs), and humans along with the vaccines and antiviral treatments^{30,31}. The cumulative cases are displayed in Fig. 1.

Clinical description and estimation procedure of parameters

Some of the NiV epidemic model embedded parameters are estimation from the clinical facts during 2001–2015 outbreaks occurred in Bangladesh. While the rest are considered from the references mentioned in the Table 1. The life expectancy of the population in Bangladesh is reported to be 73.57 years³². Consequently, the natural death rate, denoted as d_h , is calculated as $d_h = \frac{1}{365 \times 73.57}$ per day. The infection induced rate concern to NiV in Bangladesh is notably high, between 73% to 77%, while the reported recovery rate stands at 22.457%³³. Consequently, the NiV-induced death rate is estimated to be approximately $d_1 = 0.77$, and the recovery rate is estimated as $\alpha_1 = 0.22457$ ³³. Λ_h is determined using the fact $\Lambda_h = N_h(0) \times d_h$, where $N_h(0)$ represents the total population size in Bangladesh during 2015³⁴. Following same procedure, the rest of parameters can be estimated utilizing their clinical facts and reported cases as summarized in Table 1.

Model validation with real data

This section presents the fitting procedure of the proposed model with real data set given in³⁴. A robust method called the stranded nonlinear least squares regression minimization procedure is utilized for the fitting purpose. This approach is employed to identify the optimum parameter' values minimizing the error between the model simulated data and the reported data, as detailed in³⁵. The minimization process is executed using MATLAB version R2020b, utilizing the “lsqcurvefit” algorithm based on the following relation

$$\hat{\Theta} = \operatorname{argmin} \sum_{j=1}^n (H_{I_{t_j}} - \bar{H}_{I_{t_j}})^2,$$

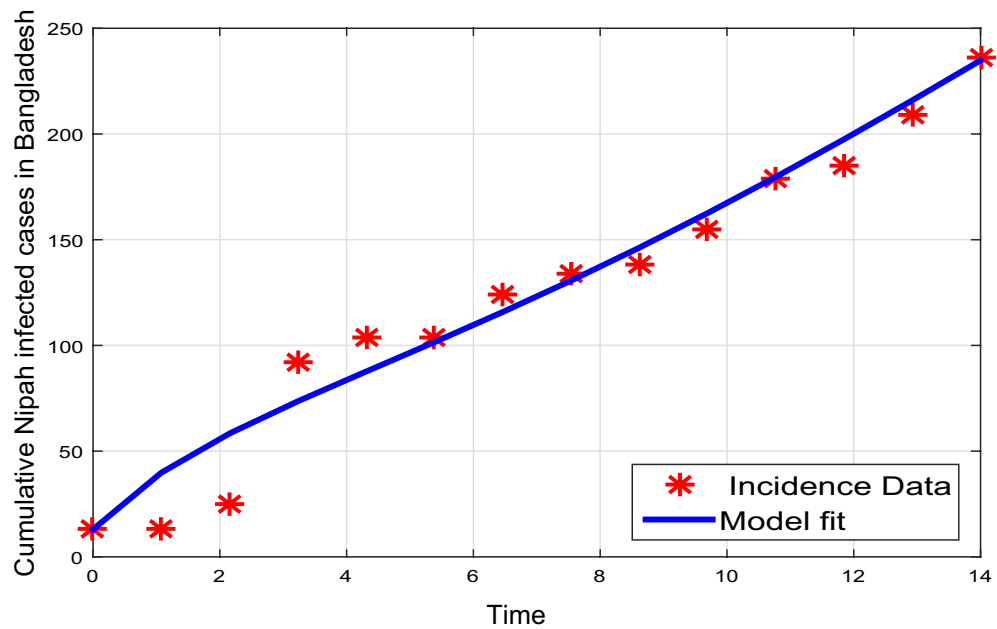


Figure 2. Model fitting curve (blue solid plot) versus real data (stars red).

Parameter	Description	Value	Reference
Λ_h	Rate of recruitment of susceptible humans	6295.17	Estimated ³⁶
Λ_f	Rate of recruitment of S_f class	300.1	³⁷
d_h	Human natural death rate	$\frac{1}{73.37 \times 365}$	Estimated ³⁶
d_f	flying foxes natural death rate	0.0250	³⁷
ν	Rate of cremation/burial of deceased	0.50	³⁸
p	Virus production rate in I_f	0.471	Fitted
θ	Decay rate of virus	0.090	Fitted
γ	Reduction in immunity	0.850	³⁸
β_1	The rate of infection of S_f	0.291	Fitted
β_2	The rate of infection of S_h	0.650	³⁷
β_3	Interaction rate between S_h and infected humans	0.750	³⁸
β_4	Interaction rate between S_h and dead bodies	0.650	³⁸
α_1	Recovery rate from contaminated class	0.090	³⁸
α_2	Recovery rate from treated class	0.090	Fitted
d_1	NiV-induced induced death rate	0.770	³⁹
κ	Ratio of contact rate of S_h with dead bodies	0.350	³⁷
ρ	Flow from infected class to treated class	0.4	³⁹
ζ	Vaccine wanning rate	0.005	Assumed
ξ	Rate of vaccinated individuals from susceptible class	0.060	Assumed

Table 1. Description of the used parameters in NiV model.

where, $\bar{H}_j t_j$ denotes real data and $H_j t_j$ are the simulated cases at temporal point t_j , whereas n denotes the entire data points. The cumulative cases are displayed in Fig. 1 while the simulated fitted curve is depicted in Fig. 2.

Sensitivity of the threshold parameters

This section presents a normalized sensitivity analysis, one of the useful tools in epidemiology and can suggest optimal control measures for an infection outbreak. We perform this analysis for various model parameters versus the reproduction number using the parametric technique⁴⁰. The purpose of sensitivity indices is to show the impact level of corresponding parameters on the infection incidence and control. The following definition is taken into account for the aforementioned purpose.

Parameter	Indices relative to \mathcal{R}_f^0	Indices relative to \mathcal{R}_h^0
β_1	1	
p	1	
d_f	-1	
θ	-1	
β_3		0.6816
β_4		0.3184
ρ		-0.3175
α_1		-0.1026
d_1		-0.2927
v		-0.3184
κ		0.3174

Table 2. Sensitivity indices of model parameters.

Definition 1 The procedure to evaluate the normalized forward sensitivity index is given by the following formula

$$Y_x = \frac{x}{\mathcal{R}_0} \frac{\partial \mathcal{R}_0}{\partial x}. \tag{25}$$

Table 2 shows the normalized sensitivity index for \mathcal{R}_h^0 and \mathcal{R}_f^0 with respect to the model parameters, using the procedure applied on (25). The sensitivity index values indicate whether a parameter has a positive or negative effect on the basic reproduction number. This helps in understanding the direct and indirect relationships between the model parameters and the basic reproduction number.

The parameters $\beta_1, p, \beta_3, \beta_4$ and κ have positive indices, indicating that they have a direct impact on \mathcal{R}_h^0 and \mathcal{R}_f^0 . This means that when these parameters increase, \mathcal{R}_h^0 and \mathcal{R}_f^0 values will increase too. Conversely, the parameters $d_f, \theta, d_1, \alpha_1, v$, and d_1 have negative indices, which suggest that they have an inverse relationship with the basic reproduction number. Therefore, if we increase these parameters, \mathcal{R}_h^0 and \mathcal{R}_f^0 values will decrease.

Furthermore, Fig. 3 shows the sensitivity indices of the model parameters as a bar graph. This graph emphasizes how crucial it is to increase treatment strategies, decrease effective contact rates between vulnerable and infected populations, and improve vaccine efficacy in order to lower the incidence of disease.

Formulation of the optimal control NiV model

We introduced six control variables in the NiV model presented in (11) for the population-level mitigation of the infection. These six control measures, namely u_1, u_2, u_3, u_4, u_5 , and u_6 , have been implemented in the model (11) to ensure its effectiveness. Each control measure plays a significant role in achieving our goals, and we have

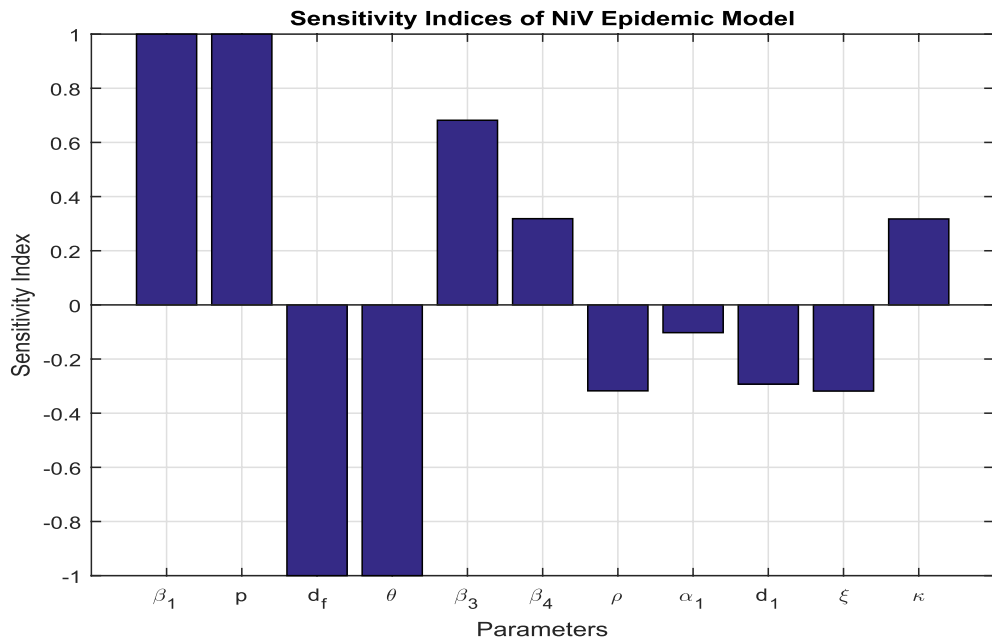


Figure 3. Bar plot showing the sensitivity indices for the NiV epidemic model.

provided a brief overview of their roles below: The control variables implemented in the NiV model serve specific purposes to control the disease incidence at the population level. The variable u_1 minimizes the transmission of viruses between susceptible flying foxes by restricting their movement with protective coverings. The variable u_2 aims to increase the mortality rate of infected Pteropus flying foxes by targeted culling particularly in areas where outbreaks have been identified. The variable u_3 manages the zoonotic transmission of viruses from infected flying foxes to humans through food contamination. The variable u_4 controls the transmission of infectious diseases by managing human contact with infected individuals and contaminated cadavers through personal protections. The variable u_5 focuses on implementing strategies to increase the number of individuals who have received NiV vaccinations. The variable u_6 measures the effort required to provide health treatment to those who are infected.

The structure of system (11) by incorporating the above control variables is given below:

$$\begin{cases} S'_f(t) = \Lambda_f - \frac{\beta_1 V(1-u_1)}{N_f} S_f - d_f S_f, \\ I'_f(t) = \frac{\beta_1 V(1-u_1)}{N_f} S_f - (d_f + u_2) I_f, \\ V'(t) = p I_f - \theta V, \\ S'_h(t) = \Lambda_h - \frac{\beta_2 V(1-u_3)}{N_h} S_h - \frac{(\beta_3 I_h + \beta_4 \kappa D_h)(1-u_4)}{N_h} S_h - (d_h + u_5) S_h + \gamma R_h + \zeta V_h, \\ V'_h(t) = u_5 S_h - (\zeta + d_h) V_h, \\ I'_h(t) = \frac{\beta_2 V(1-u_3)}{N_h} S_h + \frac{(\beta_3 I_h + \beta_4 \kappa D_h)(1-u_4)}{N_h} S_h - (u_6 + \alpha_1 + d_1 + d_h) I_h, \\ T'_h(t) = u_6 I_h - (\alpha_2 + d_h) T_h, \\ R'_h(t) = \alpha_1 I_h + \alpha_2 T_h - (\gamma + d_h) R_h, \\ D'_h(t) = d_1 I_h - \nu D_h, \end{cases} \tag{26}$$

with the ICs stated in (12). The aim of optimal control problem is to reduce the density of infected flying foxes and infected humans in class I_f and I_h , respectively, while maximizing the the vaccinated and under treatment humans. In order to accomplish this, we have formulated the following objective functional:

$$J(u_1, u_2, u_3, u_4, u_5, u_6) = \int_0^T (A_1 I_f + A_2 V + A_3 I_h + \frac{1}{2}(a_1 u_1^2 + a_2 u_2^2 + a_3 u_3^2 + a_4 u_4^2 + a_5 u_5^2 + a_6 u_6^2)) dt, \tag{27}$$

subject to problem (26). In the objective functional (27). The constants A_1, A_2, A_3 are associated weight constants while a_1, a_2, a_3, a_4, a_5 , and a_6 represent the associated cost factors. The final step size is represented by T^{41} . Our main goal is to find the optimal controls for $u_1^*, u_2^*, u_3^*, u_4^*, u_5^*$ and u_6^* , so that we can achieve our objective.

$$J(u_1^*, u_2^*, u_3^*, u_4^*, u_5^*, u_6^*) = \min\{J(u_1, u_2, u_3, u_4, u_5, u_6), (u_1, u_2, u_3, u_4, u_5, u_6) \in U\}. \tag{28}$$

The system described by Eq. (26) must satisfy certain constraints, and the control set is stated as follows:

$$U = \{(u_1, u_2, u_3, u_4, u_5, u_6) | u_i(t) \text{ is Lebesgue' Measurable on } [0, 1], i = 1, 2, 3, 4, 5, 6\}. \tag{29}$$

To solve an optimum control problem, we use Pontryagin's Principle⁴². This principle helps us formulate the necessary conditions and solutions for the problem. To begin solving the optimal problem, we focus on the Lagrangian and Hamiltonian for Eqs. (26) to (28). The Lagrangian for the optimal problem is defined as follows:

$$L = A_1 I_f + A_2 V + A_3 I_h + \frac{1}{2}(a_1 u_1^2 + a_2 u_2^2 + a_3 u_3^2 + a_4 u_4^2 + a_5 u_5^2 + a_6 u_6^2). \tag{30}$$

Our goal is to find the minimum value of the Lagrangian L mentioned above. To achieve this, we introduce the Hamiltonian function \mathbb{H} defined as follows:

$$\mathbb{H} = L + \lambda_1 \frac{dS_f}{dt} + \lambda_2 \frac{dI_f}{dt} + \lambda_3 \frac{dV}{dt} + \lambda_4 \frac{dS_h}{dt} + \lambda_5 \frac{dV_h}{dt} + \lambda_6 \frac{dI_h}{dt} + \lambda_7 \frac{dT_h}{dt} + \lambda_8 \frac{dR_h}{dt} + \lambda_9 \frac{dD_h}{dt}. \tag{31}$$

\mathbb{H} is associated with the adjoint variables $\lambda_1, \dots, \lambda_9$. In the next step, we will demonstrate that an optimal control exists for system (26).

Existence of the optimal control problem

To establish the existence of the optimal control problem, we utilize the procedure outlined in⁴³, along with the method employed by Ngina et al. in⁴⁴. We then present the following result.

Theorem 6 Consider the objective function as define above

$$J(u_1, u_2, u_3, u_4, u_5, u_6) = \int_0^T (A_1 I_f + A_2 V + A_3 I_h + \frac{1}{2}(a_1 u_1^2 + a_2 u_2^2 + a_3 u_3^2 + a_4 u_4^2 + a_5 u_5^2 + a_6 u_6^2)) dt,$$

corresponding to state and controls variables mentioned in the system (26) and satisfies the ICs

$$\begin{cases} S_f(0) = S_{f0} \geq 0, I_f(0) = I_{f0} \geq 0, V(0) = V_0 \geq 0, S_h(0) = S_{h0} \geq 0, V_h(0) = V_{h0} \geq 0, \\ I_h(0) = I_{h0} \geq 0, T_h(0) = T_{h0} \geq 0, R_h(0) = R_{h0} \geq 0, D_h(0) = D_{h0} \geq 0. \end{cases}$$

then there exists optimal controls $(u_1^*, u_2^*, u_3^*, u_4^*, u_5^*, u_6^*)$ such that

$$J(u_1^*, u_2^*, u_3^*, u_4^*, u_5^*, u_6^*) = \min\{J(u_1, u_2, u_3, u_4, u_5, u_6) | (u_1, u_2, u_3, u_4, u_5, u_6) \in U\}.$$

Proof In order to establish the existence of the said problem, we need to satisfy the following steps:

- (i) The control set U paired with each state variable equation is not empty. This condition is met as all control and state variables within U are non-empty and non-negative, and $u_i, i = 1, 2, 3, 4, 5, 6$, is a Lebesgue integrable function on the interval $[0, T]$.
- (ii) The control set is both convex as well as closed. This has been demonstrated using the methodology outlined by Ngina et al.⁴⁴. Initially, we represent the elements U in the following vector form.

$$\hat{U} = (u_1, u_2, u_3, u_4, u_5, u_6), \text{ for } 0 \leq u_1, u_2, u_3, u_4, u_5, u_6 \leq 1. \tag{32}$$

To prove the convexity of set U , let's consider constants $\varepsilon = \varepsilon_1, \varepsilon_2, \varepsilon_3, \varepsilon_4, \varepsilon_5, \varepsilon_6$ that belong to the control set U , with the condition $0 \leq \varepsilon_1, \varepsilon_2, \varepsilon_3, \varepsilon_4, \varepsilon_5, \varepsilon_6 \leq 1$.

We aim to prove that the equation

$$\omega = \phi U + (1 - \phi)\varepsilon, \text{ for } 0 \leq \phi \leq 1$$

is a part of the control set U . Therefore, our objective is to demonstrate that

$$\begin{aligned} \omega &= \phi(u_1, u_2, u_3, u_4, u_5, u_6) + (1 - \phi)(\varepsilon_1, \varepsilon_2, \varepsilon_3, \varepsilon_4, \varepsilon_5, \varepsilon_6), \\ &= (\phi u_1 + (1 - \phi)\varepsilon_1, \phi u_2 + (1 - \phi)\varepsilon_2, \phi u_3 + (1 - \phi)\varepsilon_3, \phi u_4 + (1 - \phi)\varepsilon_4, \\ &\quad \phi u_5 + (1 - \phi)\varepsilon_5, \phi u_6 + (1 - \phi)\varepsilon_6), \\ &= (\omega_1, \omega_2, \omega_3, \omega_4, \omega_5, \omega_6), \end{aligned} \tag{33}$$

where, $\omega_1 = \phi u_1 + (1 - \phi)\varepsilon_1$, is within the interval $[0, 1]$, hence, $0 \leq \omega_1 \leq 1$.

The same applies for all $\omega_2, \omega_3, \omega_4, \omega_5, \omega_6$. Hence, the vector $\omega = (\omega_1, \omega_2, \omega_3, \omega_4, \omega_5, \omega_6)$ fulfills condition (32) for convexity, establishing the convex and closed nature of the control set U .

- (iii) The boundedness of each right-hand side of (26) is a linear function of U varying with time and state variables. To establish this, we are employing the approach introduced by^{44,45}. Let

$$\dot{\Upsilon} = W\Upsilon + N(\Upsilon), \tag{34}$$

where $\Upsilon = (S_f, I_f, V, S_h, V_h, I_h, T_h, R_h, D_h)^T$,

$$W = \begin{bmatrix} -d_f & 0 & 0 & 0 & 0 & 0 & 0 & 0 & 0 & 0 \\ 0 & -d_f & 0 & 0 & 0 & 0 & 0 & 0 & 0 & 0 \\ 0 & 0 & -\theta & 0 & 0 & 0 & 0 & 0 & 0 & 0 \\ 0 & 0 & 0 & -d_h & 0 & 0 & 0 & 0 & 0 & 0 \\ 0 & 0 & 0 & 0 & -d_h & 0 & 0 & 0 & 0 & 0 \\ 0 & 0 & 0 & 0 & 0 & -d_h & 0 & 0 & 0 & 0 \\ 0 & 0 & 0 & 0 & 0 & 0 & -d_h & 0 & 0 & 0 \\ 0 & 0 & 0 & 0 & 0 & 0 & 0 & -d_h & 0 & 0 \\ 0 & 0 & 0 & 0 & 0 & 0 & 0 & 0 & -d_h & 0 \\ 0 & 0 & 0 & 0 & 0 & 0 & 0 & 0 & 0 & -\nu \end{bmatrix} \tag{35}$$

and

$$N(\Upsilon) = \begin{bmatrix} \Lambda_f - \frac{\beta_1 V(1-u_1)}{N_f} S_f \\ \frac{\beta_1 V(1-u_1)}{N_f} S_f - u_2 I_f \\ p I_f \\ \Lambda_h - \frac{\beta_2 V(1-u_3)}{N_h} S_h - \frac{(\beta_3 I_h + \beta_4 \kappa D_h)(1-u_4)}{N_h} S_h - u_5 S_h + \gamma R_h + \zeta V_h \\ u_5 S_h - \zeta V_h \\ \frac{\beta_2 V(1-u_3)}{N_h} S_h + \frac{(\beta_3 I_h + \beta_4 \kappa D_h)(1-u_4)}{N_h} S_h - (u_6 + \alpha_1 + d_1) I_h \\ u_6 I_h - \alpha_2 T_h \\ \alpha_1 I_h + \alpha_2 T_h - \gamma R_h \\ d_1 I_h \end{bmatrix}. \tag{36}$$

Representing

$$G(\Upsilon) = W\Upsilon + N(\Upsilon), \tag{37}$$

the second term, $N(\Upsilon)$ in Eq. (37) satisfies

$$\begin{aligned} |N(\Upsilon_1) - N(\Upsilon_2)| &\leq g_1 |S_{f1} - S_{f2}| + g_2 |I_{f1} - I_{f2}| + g_3 |V_1 - V_2| + g_4 |S_{h1} - S_{h2}| + g_5 |V_{h1} - V_{h2}| \\ &\quad + g_6 |I_{h1} - I_{h2}| + g_7 |T_{h1} - T_{h2}| + g_8 |R_{h1} - R_{h2}| + g_9 |D_{h1} - D_{h2}| \\ &\leq g[|S_{f1} - S_{f2}| + |I_{f1} - I_{f2}| + |V_1 - V_2| + |S_{h1} - S_{h2}| + |V_{h1} - V_{h2}| \\ &\quad + |I_{h1} - I_{h2}| + |T_{h1} - T_{h2}| + |R_{h1} - R_{h2}| + |D_{h1} - D_{h2}|], \end{aligned} \tag{38}$$

where

$$\Upsilon_1 = (S_{f1}, I_{f1}, V_1, S_{h1}, V_{h1}, I_{h1}, T_{h1}, R_{h1}, D_{h1}), \Upsilon_2 = (S_{f2}, I_{f2}, V_2, S_{h2}, V_{h2}, I_{h2}, T_{h2}, R_{h2}, D_{h2})$$

and g is an independent constant such that

$$g = \max(g_i, i = 1, \dots, 9).$$

Also,

$$|G(\Upsilon_1) - G(\Upsilon_2)| \leq g|\Upsilon_1 - \Upsilon_2|, \text{ where } g = \sum_{i=1}^9 g_i + \|G\| \leq \infty.$$

The function $G(\Upsilon)$ is uniformly Lipschitz continuous, given the definitions of the control variables $u_1(t), u_2(t), u_3(t), u_4(t), u_5(t), u_6(t)$ and the constraints on the state variables;

$$(S_f > 0, I_f \geq 0, V \geq 0, S_h \geq 0, V_h \geq 0, I_h \geq 0, T_h \geq 0, R_h \geq 0, D_h \geq 0),$$

Consequently, the solution of the system (26) exists, thereby concluding the proof third condition.

(iv) The integrand in (27) provided by

$$\mathcal{P} = A_1 I_f + A_2 V + A_3 I_h + \frac{1}{2}(a_1 u_1^2 + a_2 u_2^2 + a_3 u_3^2 + a_4 u_4^2 + a_5 u_5^2 + a_9 u_6^2) \tag{39}$$

exhibits convexity with respect to U . To establish this property, we employ the Hessian matrix method, defined as below:

Definition 6.1

Given a function $\mathcal{V}(y_1, y_2, y_3, \dots, y_n)$, of several variables, then \mathcal{V} , will be convex if and only if the Hessian matrix, H_m is such that

$$H_m(y) = \left[\frac{\partial^2 \mathcal{V}}{\partial y_i \partial y_j} \right] \geq 0, \forall y \neq 0,$$

and it is considered to be concave if and only if

$$H_m(y) = \left[\frac{\partial^2 \mathcal{V}}{\partial y_i \partial y_j} \right] \leq 0, \forall y \neq 0.$$

So let

$$\mathcal{P}_i = \frac{1}{2}(a_1 u_1^2 + a_2 u_2^2 + a_3 u_3^2 + a_4 u_4^2 + a_5 u_5^2 + a_6 u_6^2),$$

where $\mathcal{P}_i \in \mathcal{P}$, the Hessian Matrix for \mathcal{P}_i is given by

$$H_m = \begin{bmatrix} a_1 & 0 & 0 & 0 & 0 & 0 \\ 0 & a_2 & 0 & 0 & 0 & 0 \\ 0 & 0 & a_3 & 0 & 0 & 0 \\ 0 & 0 & 0 & a_4 & 0 & 0 \\ 0 & 0 & 0 & 0 & a_5 & 0 \\ 0 & 0 & 0 & 0 & 0 & a_6 \end{bmatrix} \geq 0, \text{ for } a_1, a_2, a_3, a_4, a_5, a_6 \geq 0. \tag{40}$$

It can be observed that \mathcal{P}_i is a convex function in the domain U . If $\mathcal{P}_i \in \mathcal{P}$ is convex in U , then it implies that \mathcal{P} is also convex in U and satisfies condition (iv).

(xxii) Additionally, there exist some constants $n_1, n_2 > 0$, and $n_3 > 1$, such that the integrand of (39) is both convex and bounded by

$$\mathcal{P}(t, S_f, I_f, V, S_h, V_h, I_h, T_h, R_h, D_h, u_1, u_2, u_3, u_4, u_5, u_6) \leq n_2 - \frac{n_1}{2} \left(\sum_{i=1}^6 |u_i|^2 \right)^{\frac{n_3}{2}}.$$

From (27), we proceed as

$$J(u_1(t), u_2(t), u_3(t), u_4(t), u_5(t), u_6(t)) = A_1 I_f + A_2 V + A_3 I_h + \frac{1}{2} \left(\sum_{i=1}^6 a_i u_i^2 \right),$$

then,

$$J(u_1(t), u_2(t), u_3(t), u_4(t), u_5(t), u_6(t)) \leq A_1 I_f + A_2 V + A_3 I_h + \sum_{i=1}^6 a_i u_i^2. \tag{41}$$

Letting $a = \max(a_1, a_2, a_3, a_4, a_5, a_6)$ such that

$$J(u_1(t), u_2(t), u_3(t), u_4(t), u_5(t), u_6(t)) \leq A_1 I_f + A_2 V + A_3 I_h + a \sum_{i=1}^6 u_i^2, \tag{42}$$

this means that

$$A_1 I_f + A_2 V + A_3 I_h + \sum_{i=1}^6 a_i u_i^2 \leq n_2 + n_1 \sum_{i=1}^6 |u_i|^2, \tag{43}$$

where n_2 based on the upper bound on I_f, V, I_h and $n_1 > 0$ since $a_i > 0$ for $i = 1, \dots, 6$. Therefore, Eq. (42) can be revised as

$$J(u_1, u_2, u_3, u_4, u_5, u_6) \leq n_2 + n_1(u_1, u_2, u_3, u_4, u_5, u_6)^2. \tag{44}$$

Now, from Eq. (44), it is observed that $n_1, n_2 > 0$, and $n_3 = 2 > 1$. Finally, we conclude that there must exists an optimal control variables $u_1^*, u_2^*, u_3^*, u_4^*, u_5^*, u_6^*$. This completes the proof. \square

$$\begin{cases} z' = \frac{\partial \mathbb{H}(t, z, u, \lambda)}{\partial z}, \\ 0 = \frac{\partial \mathbb{H}(t, z, u, \lambda)}{\partial u}, \\ \lambda' = \frac{\partial \mathbb{H}(t, z, u, \lambda)}{\partial \lambda}. \end{cases} \tag{45}$$

To obtain the necessary results, we use the above described conditions as follow.

Theorem 7 Let $S_f^*, I_f^*, V^*, S_h^*, V_h^*, I_h^*, T_h^*, R_h^*$, and D_h^* represent the state solutions associated with the optimal control measures $u_1^*, u_2^*, u_3^*, u_4^*, u_5^*$, and u_6^* for the optimum control system stated in (26) and (27). Then, we find the adjoint variables $\lambda_1, \dots, \lambda_9$ that satisfy:

$$\left\{ \begin{aligned} \lambda'_1 &= d_f \lambda_1 + (\lambda_2 - \lambda_1) \frac{S_f V \beta_1 (1-u_1)}{N_f^2} + (\lambda_1 - \lambda_2) \frac{V \beta_1 (1-u_1)}{N_f}, \\ \lambda'_2 &= -A_3 + (\lambda_6 - \lambda_7) u_6 + (\lambda_6 - \lambda_8) \alpha_1 - \lambda_9 (d_1 + d_h) + (\lambda_6 - \lambda_4) \frac{S_h I_h \beta_2 (1-u_3)}{N_h^2} \\ &\quad + (\lambda_4 - \lambda_6) \frac{(S_h I_h) \beta_2 (1-u_3)}{N_h} + (\lambda_4 - \lambda_6) \frac{S_h \beta_3 (1-u_4)}{N_h} + (\lambda_6 - \lambda_4) \frac{S_h (\beta_3 I_h + \beta_4 \kappa D_h) (1-u_4)}{N_h^2}, \\ \lambda'_3 &= \theta \lambda_3 + (\lambda_1 - \lambda_2) \frac{S_f \beta_1 (1-u_1)}{N_f}, \\ \lambda'_4 &= d_h \lambda_4 + (\lambda_4 - \lambda_5) u_5 + (\lambda_6 - \lambda_4) \frac{\beta_2 S_h I_h (1-u_3)}{N_h^2} + (\lambda_4 - \lambda_6) \frac{\beta_2 I_h (1-u_3)}{N_h} \\ &\quad + (\lambda_6 - \lambda_4) \frac{S_h (\beta_3 I_h + \beta_4 \kappa D_h)}{N_h^2} + (\lambda_4 - \lambda_6) \frac{(\beta_3 I_h + \beta_4 \kappa D_h) (1-u_4)}{N_h}, \\ \lambda'_5 &= -A_1 + \lambda_5 d_h + (\lambda_5 - \lambda_4) \zeta + (\lambda_6 - \lambda_4) \frac{\beta_2 S_h I_h (1-u_3)}{N_h^2} + (\lambda_6 - \lambda_4) \frac{\beta_2 S_h I_h (I_h \beta_3 + \kappa d_h \beta_4) (1-u_4)}{N_h^2}, \\ \lambda'_6 &= -A_3 + (\lambda_6 - \lambda_7) u_6 + \alpha_1 (\lambda_6 - \lambda_8) + (\lambda_6 - \lambda_9) d_1 + \lambda_6 d_h + (\lambda_6 - \lambda_4) \frac{\beta_2 S_h I_h (1-u_3)}{N_h^2} \\ &\quad + (\lambda_4 - \lambda_6) \frac{S_h \beta_2 (1-u_3)}{N_h} + (\lambda_4 - \lambda_6) \frac{S_h \beta_3 (1-u_4)}{N_h} + (\lambda_6 - \lambda_4) \frac{S_h (\beta_3 I_h + \beta_4 \kappa D_h) (1-u_4)}{N_h^2}, \\ \lambda'_7 &= -A_2 + d_h \lambda_7 + \alpha_2 (\lambda_7 - \lambda_8) + (\lambda_6 - \lambda_4) \frac{\beta_2 S_h I_h (1-u_3)}{N_h^2} + (\lambda_6 - \lambda_4) \frac{S_h (\beta_3 I_h + \beta_4 \kappa D_h) (1-u_4)}{N_h^2}, \\ \lambda'_8 &= d_h \lambda_8 + (\lambda_8 - \lambda_4) \gamma + (\lambda_6 - \lambda_4) \frac{\beta_2 S_h I_h (1-u_3)}{N_h^2} + (\lambda_6 - \lambda_4) \frac{S_h (\beta_3 I_h + \beta_4 \kappa D_h) (1-u_4)}{N_h^2}, \\ \lambda'_9 &= \nu \lambda_9 + (\lambda_4 - \lambda_6) \frac{\beta_4 \kappa S_h (1-u_4)}{N_h}, \end{aligned} \right. \tag{46}$$

with boundary conditions or transversality conditions

$$\lambda_i(T) = 0, i = 1, \dots, 9.$$

Moreover, the control measures $u_1^*, u_2^*, u_3^*, u_4^*, u_5^*$ and u_6^* are given by

$$\left\{ \begin{aligned} u_1^* &= \max \left\{ \min \left(\frac{\beta_1 S_f V (\lambda_3 - \lambda_2)}{N_f a_1}, 1 \right), 0 \right\}, \\ u_2^* &= \max \left\{ \min \left(\frac{\lambda_3 I_f}{a_2}, 1 \right), 0 \right\}, \\ u_3^* &= \max \left\{ \min \left(\frac{(\lambda_6 - \lambda_4) \beta_2 I_h S_h}{N_h a_3}, 1 \right), 0 \right\}, \\ u_4^* &= \max \left\{ \min \left(\frac{(\lambda_6 - \lambda_4) (\beta_3 I_h + \beta_4 \kappa D_h) S_h}{N_h a_4}, 1 \right), 0 \right\}, \\ u_5^* &= \max \left\{ \min \left(\frac{(\lambda_4 - \lambda_5) S_h}{a_5}, 1 \right), 0 \right\}, \\ u_6^* &= \max \left\{ \min \left(\frac{(\lambda_6 - \lambda_7) I_h}{a_6}, 1 \right), 0 \right\}. \end{aligned} \right. \tag{47}$$

Proof In order to obtain the transversality and adjoint system conditions with the correct boundary values, we utilize the Hamiltonian function \mathbb{H} , as shown in Eq. (31). By employing Pontryagin’s maximum principle, we can derive the adjoint equations in a methodical and effective way.

$$\frac{d\lambda_1(t)}{dt} = -\frac{\partial \mathbb{H}}{\partial S_f}, \frac{d\lambda_2(t)}{dt} = -\frac{\partial \mathbb{H}}{\partial I_f}, \dots, \frac{d\lambda_8(t)}{dt} = -\frac{\partial \mathbb{H}}{\partial D_h},$$

subject to boundary time conditions (i.e. final) $\lambda_i(T) = 0$ for $i = 1, 2, \dots, 9$. In order to achieve the desired problem (47), we utilize the following equations:

$$\frac{\partial \mathbb{H}}{\partial u_i} = 0, i = 1, \dots, 6.$$

By utilizing the property of the control space U being in the interior of the control set, we obtain the desired result. □

Simulation and discussion

In order to examine the effectiveness of the aforementioned control measures, we conducted a detailed numerical analysis of the NiV epidemic models with variable and constant controls given (26) and (11) respectively. Utilizing the backward fourth-order Runge-Kutta method, the model was numerically solved. The parameter’s values used in simulation are mentioned in Table 2. The balance constants and weights were adjusted to $A_1 = 01$, $A_2 = A_3 = 10$, $a_1 = a_2 = 15$, $a_3 = 10$, $a_4 = 15$, $a_5 = 10$ and $a_6 = 50$. The control profile for this scenario is represented by Fig. j in all figures. The red solid plots indicate the dynamics without control, while the black dashed trajectories depict the dynamics with optimal control. Each and every section of graphs have nine classes as: (a) Virus class (b) susceptible flying foxes (c) infected flying foxes (d) susceptible human (e) vaccinated human (f) infected human (g) treated human (h) recovered human (i) deceased human and (j) all controls.

Applying all controls simultaneously, i.e., $u_i \neq 0$, where, $i = 1, 2, 3, 4, 5, 6$

In order to analyze the effectiveness of optimal control measures in reducing infections in the NiV control model, we conducted simulations that included all suggested control interventions. The simulation demonstrated a notable decrease in the virus and the number of infected individuals among flying foxes, as well as among the

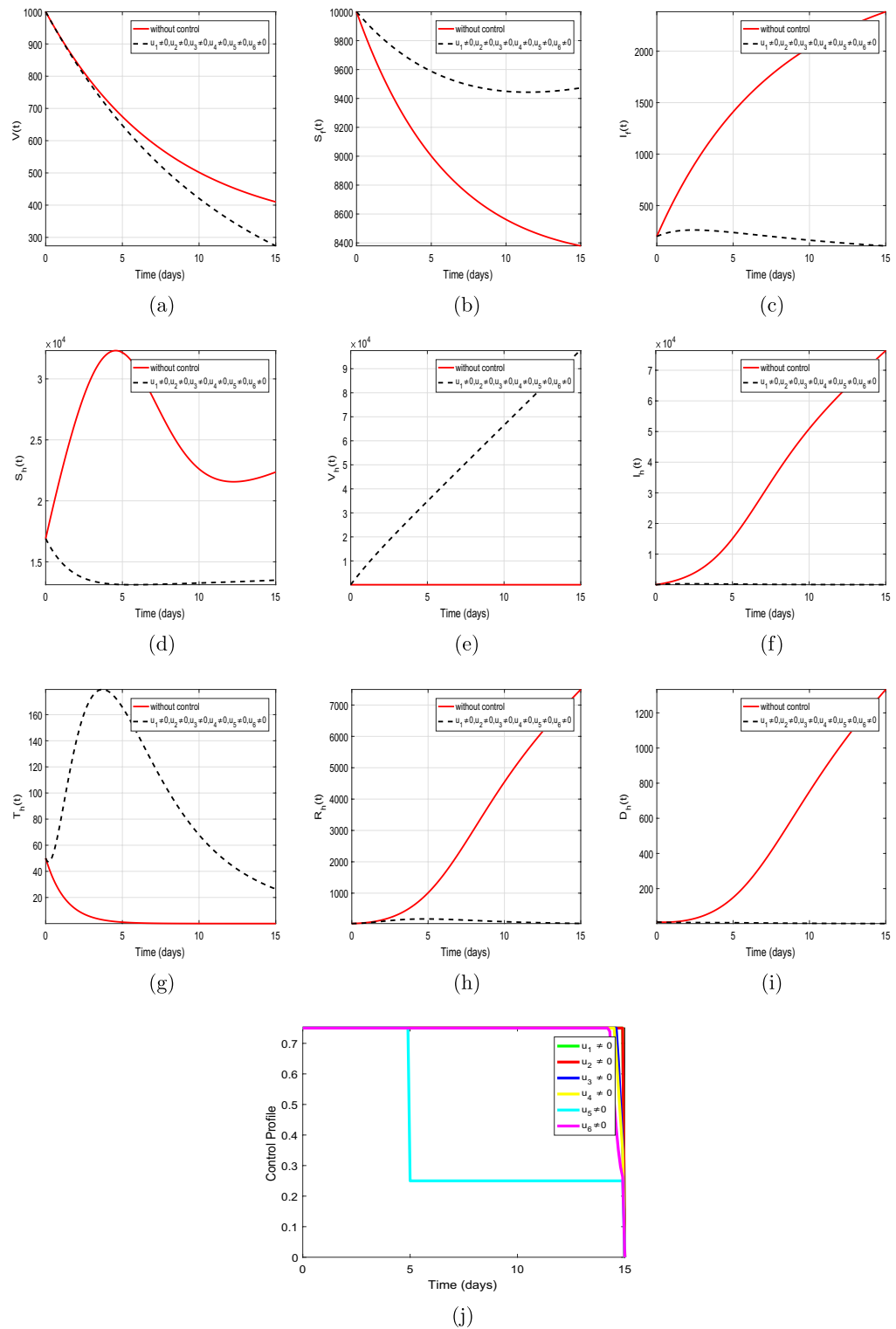


Figure 4. Usage of all control interventions.

susceptible, infected, recovered, and deceased human populations when all control measures were implemented. Conversely, the population of susceptible flying foxes, vaccinated humans, and treated human groups increased with the implementation of optimal controls. For a visual representation of the simulation dynamics, see Fig. 4. It is worth mentioning here that with the application of optimal controls, most of the population in the susceptible class are either vaccinated or protected from the virus (with other non-pharmaceutical measures) as shown in Fig. 4d,e,g, subsequently there are fewer people at risk of infection (see Fig. 4f). This reduction in risk results in fewer infection cases and, consequently, a decrease in the number of recovery cases (see Fig. 4h). The same

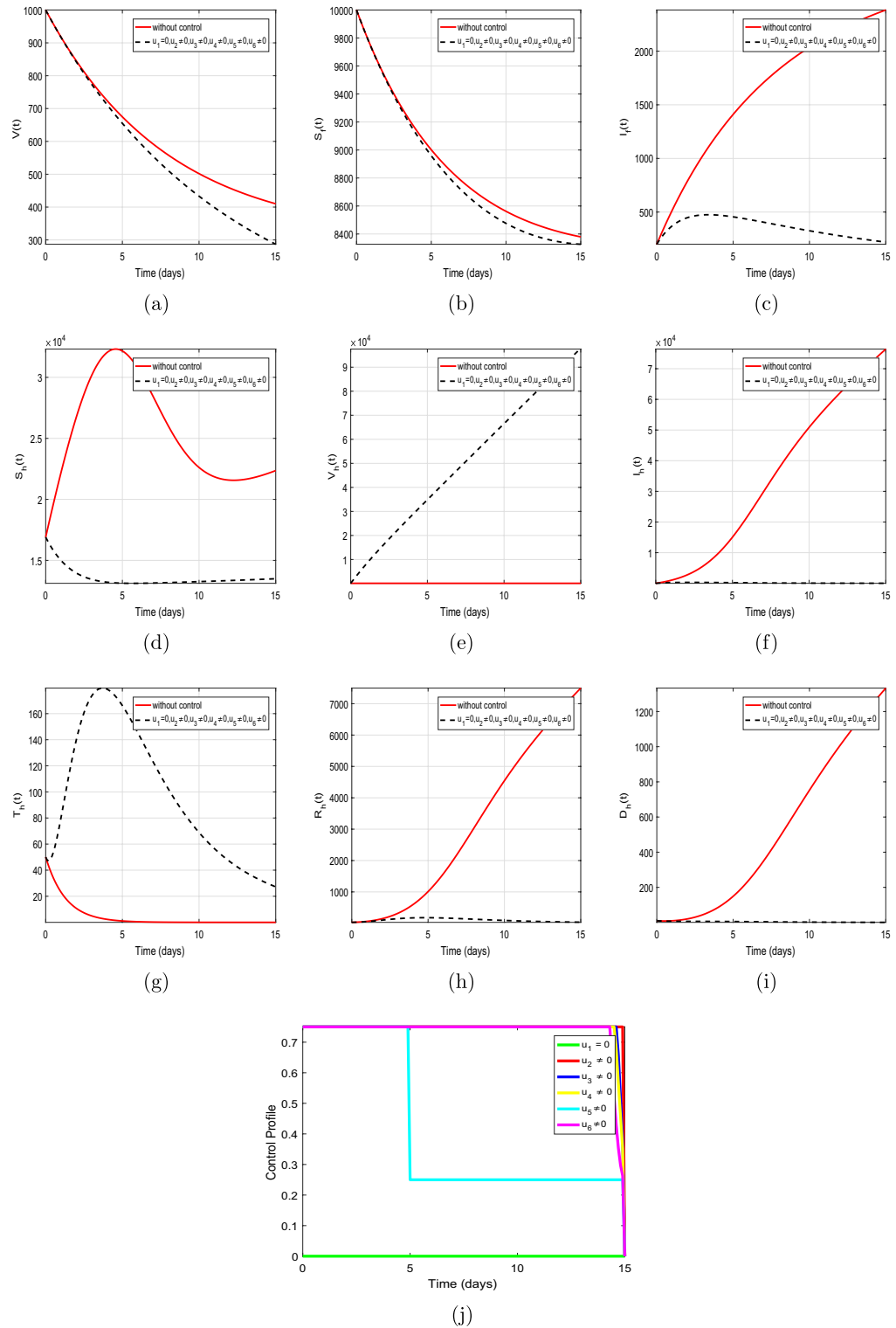


Figure 5. Usage of all controls except u_1 .

scenario is observed in all subsequent strategies. This type of behavior can also be found in previous studies, such as the one described in⁴⁶.

Second strategy: $u_1 = 0$, and $u_i \neq 0$, where, $i = 2, 3, 4, 5, 6$

In the second strategy, we simulate the NiV model by activating all control interventions simultaneously except u_1 to investigate their combined impact on the disease dynamics. The graphical representation of this scenario is illustrated in Fig. 5, which shows the dynamics of both human and flying fox populations. According to the

system (26) with control measures, there was a decrease in the virus and the susceptible and infected populations of flying foxes. Similarly, there was a significant decrease in the susceptible, infected, recovered, and deceased human populations compared to the system (11) without control measures. In contrast, the number of vaccinated and treated individuals showed a significant increase. Figure 5j displays the control profile for this scenario. The graphical findings of this strategy, both with and without control, revealed more noteworthy outcomes for the human population. Thus, control interventions can be effectively used to reduce infection.

Third strategy: $u_2 = 0$, and $u_i \neq 0$, where, $i = 1, 3, 4, 5, 6$

In the third strategy, we simulate the NiV model by activating all control interventions except u_2 simultaneously. This allows us to examine how these interventions work together to affect the disease dynamics. Figure 6 provides a graphical interpretation of this scenario, showing the dynamics of the human and flying fox populations. The results from system (26) with control measures show a decrease in the infected population of flying foxes, but an increase in susceptible flying foxes. Comparing the susceptible, recovered, infectious and deceased human individuals to the system (11) without control measures, a significant drop was observed. However, there was a notable increase in the number of people who received treatment and vaccinations. Figure 6j displays the control profile corresponding to this case. When comparing the results with and without control, it is evident that the control intervention has a more significant impact on the human population in this strategy. Therefore, control interventions can be used to effectively minimize the infection.

Fourth strategy: $u_3 = 0$, and $u_i \neq 0$, where, $i = 1, 2, 4, 5, 6$

In the fourth strategy, we examine the effects of simultaneously activating all control interventions except u_3 on the dynamics of the NiV model. This helps us understand the combined impact of control measures on the disease dynamics. Figure 7 provides a graphical illustration of this scenario, showing the dynamics of the flying fox and human populations. The results obtained from system (26) with control measures indicate a decrease in the infected population of flying foxes, but an increase in the susceptible flying foxes. Additionally, the population density in susceptible, recovered, infectious and deceased human show a significant decrease compared to the uncontrolled system (11). On the other hand, the density of vaccinated and treated classes observe a substantial increase. The corresponding control profile is depicted in Fig. 7j. The simulation in both cases reveal more significant findings for the human population, indicating that control methods can be effectively employed to reduce the infection.

Fifth strategy: $u_4 = 0$, and $u_i \neq 0$, where, $i = 1, 2, 3, 5, 6$

In the fifth strategy, we examine the NiV model by activating all control interventions except u_4 simultaneously to observe their effects on disease dynamics. Figure 8 provides a graphical interpretation of this scenario, illustrating the interactions between human and flying fox populations. The results from system (26) with control measures indicate that the virus and the infected population of flying foxes decreased, while the susceptible flying fox population increased. Additionally, the number of susceptible, infected, recovered, and deceased humans notably declined compared to the without variable controls. Conversely, the density of individuals who have received vaccinations and treatments significantly increased. Figure 8j illustrates the profile of all controls corresponding to this scenario. The simulation in both cases show more significant outcomes for the human population in this strategy, indicating that this control interventions can effectively minimize the infection.

Sixth strategy: $u_5 = 0$, and $u_i \neq 0$, where, $i = 1, 2, 3, 4, 6$

As part of strategy 6, a simulation was conducted on the NiV model by activating all control interventions except for u_5 simultaneously. This was done to observe the collective impacts on the disease dynamics. Figure 9 provides a graphical interpretation of this scenario, outlining the interactions between flying fox and human populations. The control results derived from system (26) indicate a decrease in the virus and the population of infected flying foxes, while the susceptible flying fox population increased. Similarly, in humans, the susceptible, infected, recovered, and deceased populations all saw a significant decrease compared to (11) results without control. Interestingly, the treated class dramatically enhanced, but there was no change in the number of vaccinated individuals. The control profile for this particular instance can be found in Fig. 9j. The simulation with control intervention depicts a reasonable impact on the human population in this strategy, indicating that control measures can effectively minimize the spread of the infection.

Seventh strategy: $u_6 = 0$, and $u_i \neq 0$, where, $i = 2, 3, 4, 5$

In the seventh strategy, an analysis was conducted to simulate the NiV model and examine the combined effects of all control interventions except u_6 on the disease dynamics. The simulation results, illustrated in Fig. 10, showed

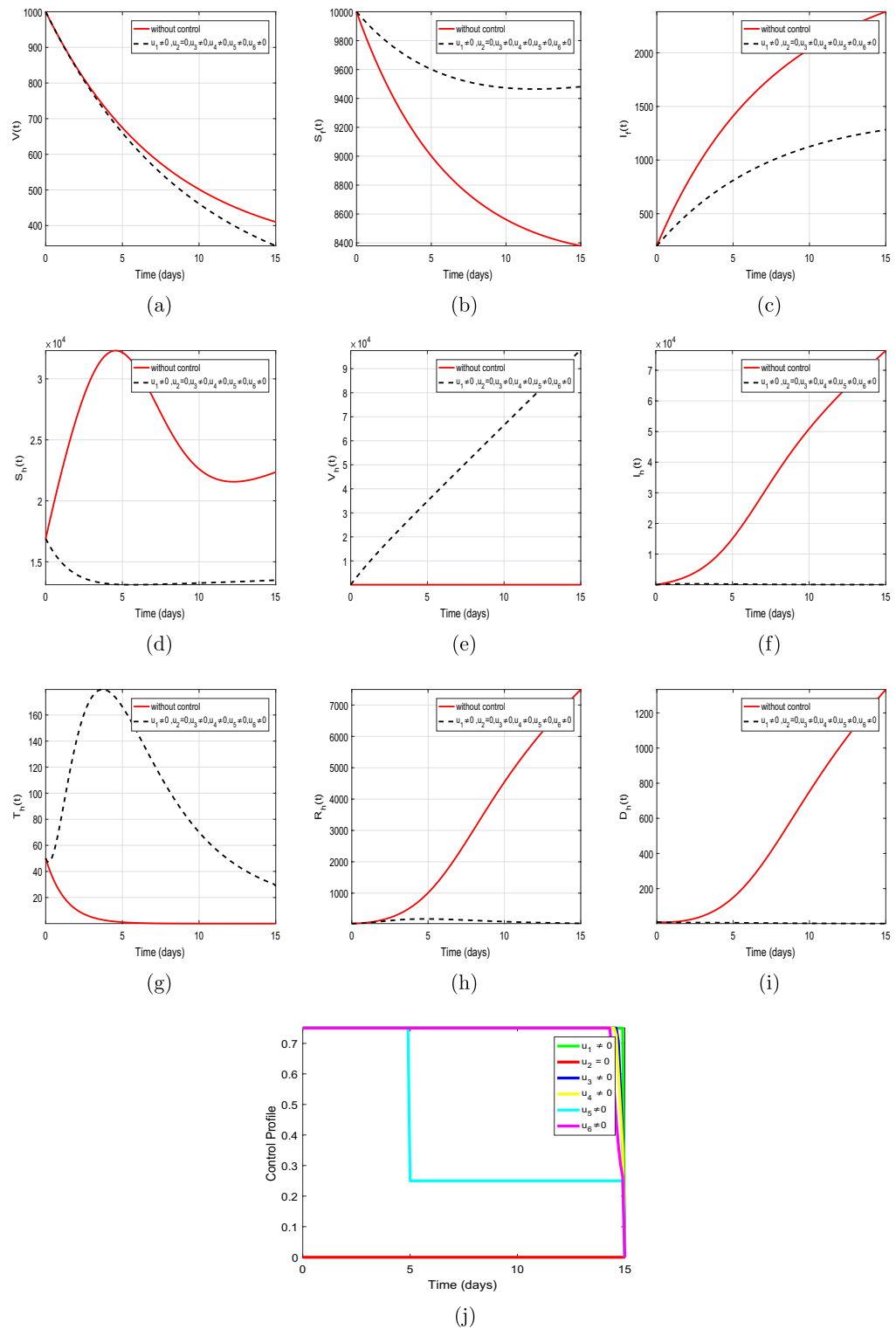


Figure 6. Impact of using all controls except u_2 .

that the infected population of flying foxes decreased, while the susceptible flying fox population increased. In humans, the susceptible, infected, recovered, and deceased populations showed a significant decrease compared to (11) results without control. Moreover, the vaccinated individuals density increased but there was no change observed in the treated individuals. The analysis of both cases i.e., with constant and time-varying strategies demonstrated a higher degree of significance in the human population under the variable strategy. These findings suggest that variable control interventions can be effectively employed to mitigate infection rates and reduce the spread of the disease.

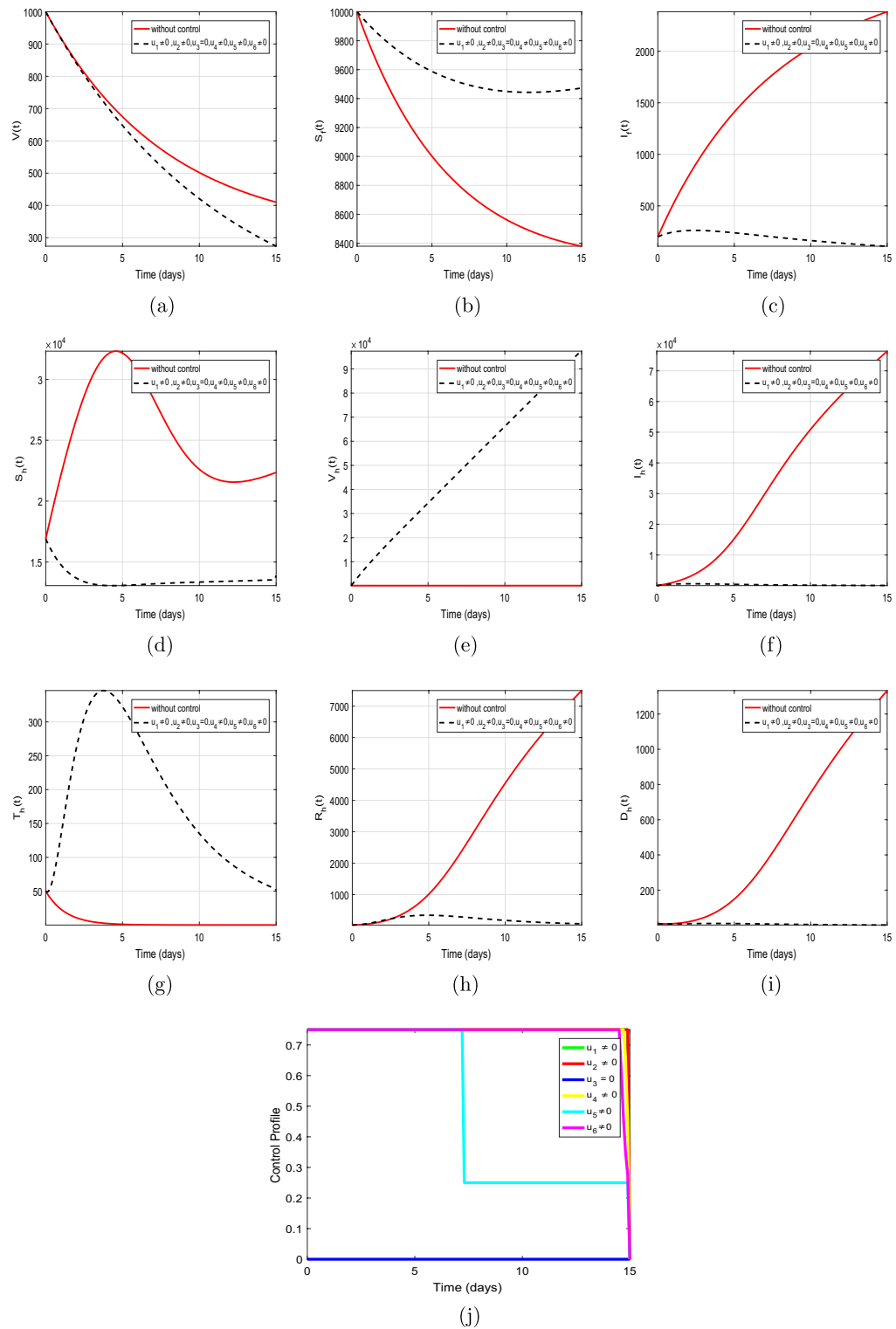


Figure 7. Impact of using all controls except u_3 .

To get a better grasp of the entire process, refer to the following table 3.

Conclusion

The aim of this study is to present a mathematical model that captures the dynamics of NiV. We developed a mathematical model that considers multiple transmission modes of the virus and combines the impact of treatment and vaccination. The model we formulated includes both human-to-human and food-borne transmissions. We presented a detailed analysis of the model and examined potential problem equilibria based on the

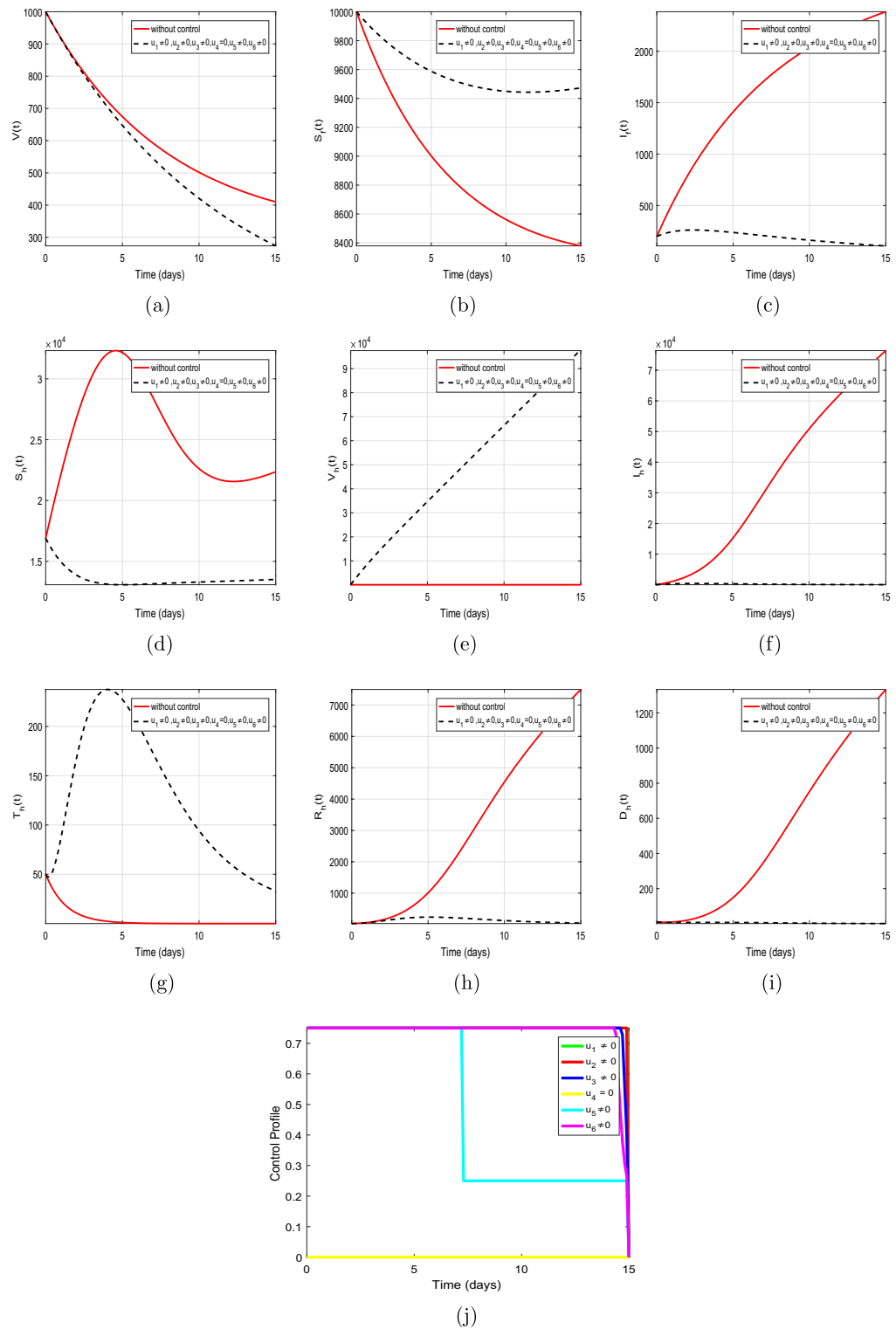


Figure 8. Impact of using all controls except u_4 .

reproduction number. It was observed that the model has three equilibrium states: disease-free, infected flying fox-free, and endemic steady state. The model was successfully applied to the reported outbreaks in Bangladesh during 2001–2015, and the parameters were estimated from clinical data. A normalized sensitivity analysis was conducted to identify the most influential parameters in the model. The analysis indicated that increasing treatment strategies, reducing effective contact rates between susceptible and infected populations, and enhancing vaccine efficacy are critical for disease eradication. Further, by incorporating six control variables, a control model was constructed based on the sensitivity analysis. We conducted extensive simulations by considering

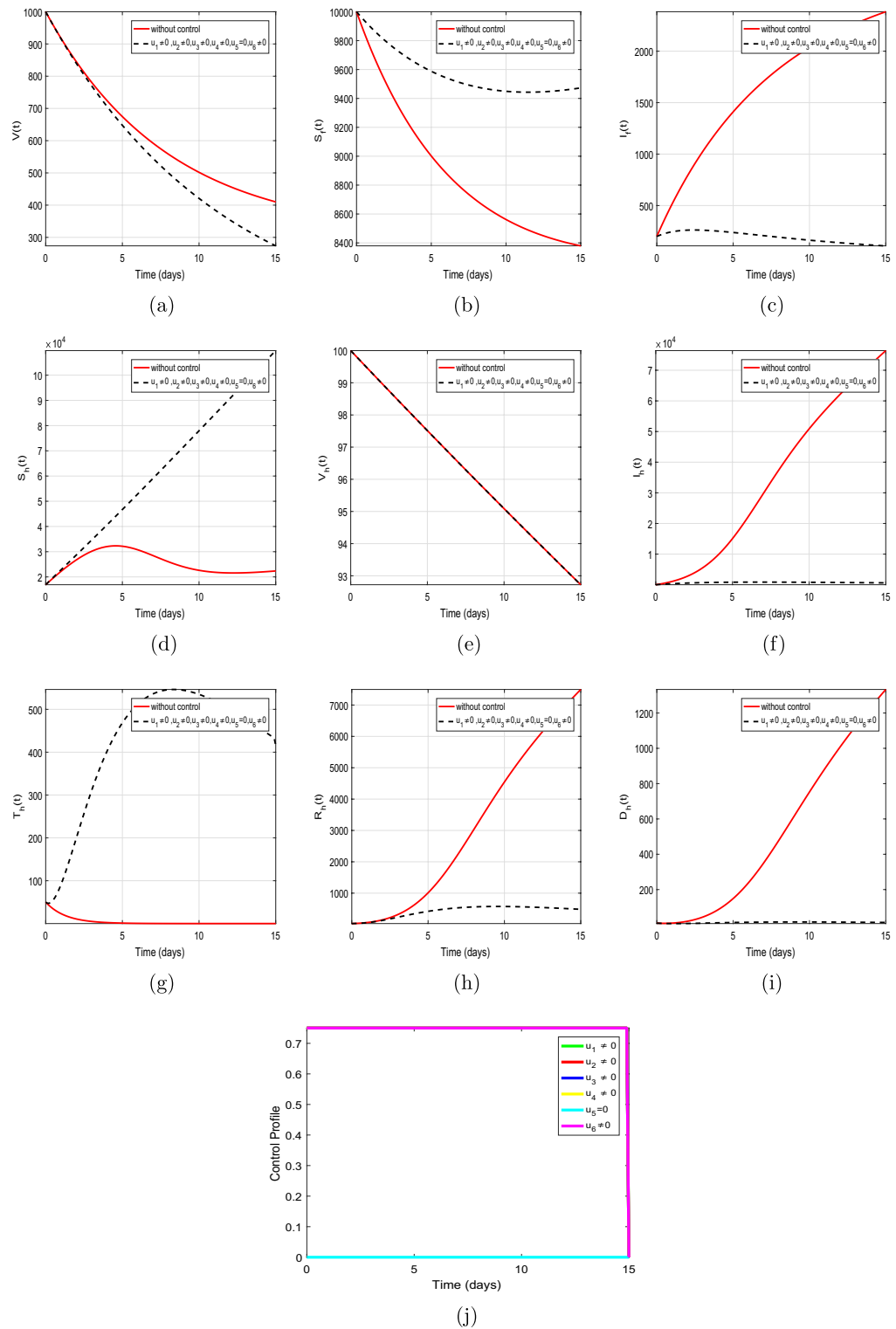


Figure 9. Impact of using all controls except u_5 .

seven different strategies. Under the optimal control strategy, the simulation demonstrated more significant results in the human population as the number of infected individuals diminished. These findings suggest that time-varying control interventions can effectively mitigate infection rates and limit the spread of the disease. In future studies, we plan to extend the proposed model using a novel fractional and fractal-fractional modeling approaches with perfect and imperfect vaccination.

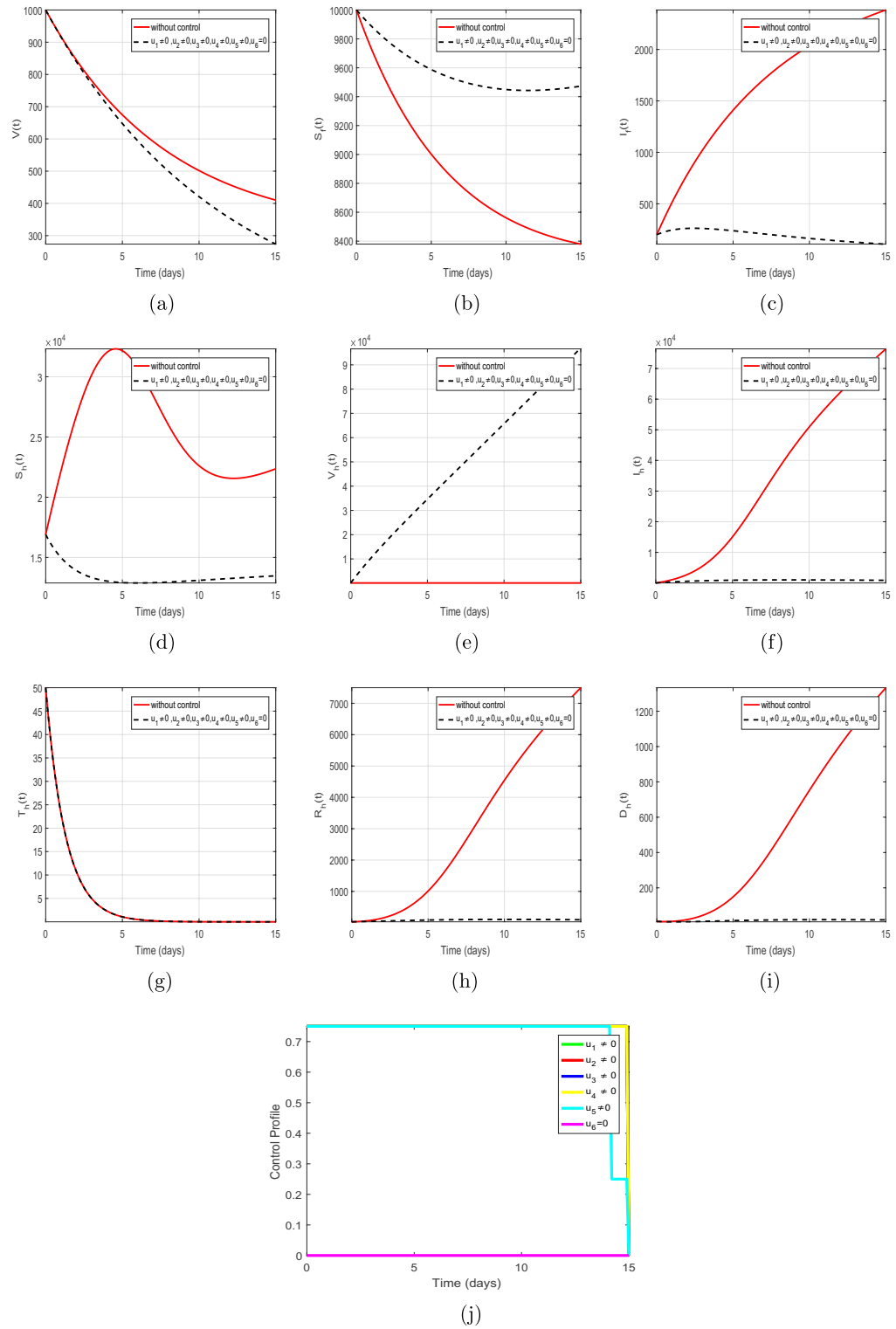


Figure 10. Impact of using all controls except u_6 .

The comprehensive process of all graphs has been illustrated in the table below.											
Case no.	Here ↓, shows decrease, ↑, increases and ⇌, no change	V	S _f	I _f	S _h	V _h	I _h	T _h	R _h	D _h	
1, see Fig. 4	If all $u_i \neq 0$, where, $i = 1, 2, 3, 4, 5, 6$	↓	↑	↓	↓	↑	↓	↑	↓	↓	
2, see Fig. 5	If $u_1 = 0$ and others $u_i \neq 0$, where, $i = 2, 3, 4, 5, 6$	↓	↓	↓	↓	↑	↓	↑	↓	↓	
3, see Fig. 6	If $u_2 = 0$ and others $u_i \neq 0$, where, $i = 1, 3, 4, 5, 6$	↓	↑	↓	↓	↑	↓	↑	↓	↓	
4, see Fig. 7	If $u_3 = 0$ and others $u_i \neq 0$, where, $i = 1, 2, 4, 5, 6$	↓	↑	↓	↓	↑	↓	↑	↓	↓	
5, see Fig. 8	If $u_4 = 0$ and others $u_i \neq 0$, where, $i = 1, 2, 3, 5, 6$	↓	↑	↓	↓	↑	↓	↑	↓	↓	
6, see Fig. 9	If $u_5 = 0$ and others $u_i \neq 0$, where, $i = 1, 2, 3, 4, 6$	↓	↑	↓	↑	⇌	↓	↑	↓	↓	
7, see Fig. 10	If $u_6 = 0$ and others $u_i \neq 0$, where, $i = 1, 2, 3, 4, 5$	↓	↑	↓	↓	↑	↓	⇌	↓	↓	

Table 3. Description of the suggested strategies.

Data availability

The data that support the findings of this study are available from the corresponding author upon reasonable request. Further, no experiments on humans and/or the use of human tissue samples involved in this study.

Received: 23 February 2024; Accepted: 19 July 2024

Published online: 30 July 2024

References

- Centers for Disease Control and Prevention, Nipah disease (2022). <https://www.cdc.gov/vhf/nipah/transmission/index.html>. Accessed May 25, 2023.
- Halpin, K. *et al.* Pteropid bats are confirmed as the reservoir hosts of henipaviruses: A comprehensive experimental study of virus transmission. *ASTMH* **85**(5), 946 (2011).
- Chattu, V. K., Kumar, R., Kumary, S., Kajal, F. & David, J. K. Nipah virus epidemic in southern India and emphasizing "One Health" approach to ensure global health security. *Fam. Med. Prim. Care Rev.* **7**(2), 275 (2018).
- Sazzad, H. M. *et al.* Nipah virus infection outbreak with nosocomial and corpse-to-human transmission, Bangladesh. *EID* **19**(2), 210 (2013).
- Chanchal, D. K., Alok, S., Sabharwal, M., Bijauliya, R. K. & Rashi, S. Nipah: Silently rising infection. *IJPSR* **9**(8), 3128–3135 (2018).
- Clayton, B. A. Nipah virus: Transmission of a zoonotic paramyxovirus. *Curr. Opin. Virol.* **22**, 97–104 (2017).
- Luby, S. P. The pandemic potential of Nipah virus. *Antiviral Res.* **100**(1), 38–43 (2013).
- Chua, K. B. *et al.* Nipah virus: A recently emergent deadly paramyxovirus. *Science* **288**(5470), 1432–1435 (2000).
- Montgomery, J. M. *et al.* Risk factors for Nipah virus encephalitis in Bangladesh. *EID* **14**(10), 1526 (2008).
- Chakraborty, A. *et al.* Evolving epidemiology of Nipah virus infection in Bangladesh: Evidence from outbreaks during 2010–2011. *Epidemiol. Infect.* **144**(2), 371–380 (2016).
- Gurley, E. S. *et al.* Person-to-person transmission of Nipah virus in a Bangladeshi community. *EID* **13**(7), 1031 (2007).
- Chadha, M. S. *et al.* Nipah virus-associated encephalitis outbreak, Siliguri, India. *EID* **12**(2), 235 (2006).
- Luo, J. *et al.* Role of perceived ease of use, usefulness, and financial strength on the adoption of health information systems: The moderating role of hospital size. *Human. Soc. Sci. Commun.* **11**(1), 516 (2024).
- Khan, M. A., Ullah, S. & Kumar, S. A robust study on 2019-nCoV outbreaks through non-singular derivative. *Eur. Phys. J. Plus* **136**, 1–20 (2021).
- Khan, F. M. & Khan, Z. U. Numerical analysis of fractional order drinking mathematical model. *J. Math. Tech. Model.* **1**(1), 11–24 (2024).
- Alzubaidi, A. M., Othman, H. A., Ullah, S., Ahmad, N. & Alam, M. M. Analysis of Monkeypox viral infection with human to animal transmission via a fractional and Fractal-fractional operators with power law kernel. *Math. Biosci. Eng.* **20**, 6666–6690 (2023).
- Fatmawati, H. F., Herdicho, F. F., Windarto, W., Chukwu, W. & Tasman, H. An optimal control of malaria transmission model with mosquito seasonal factor. *Results Phys.* **25**, 104238 (2021).
- Zhang, J., Fang, Q., Xiang, P., Sun, D., Xue, Y., Jin, R. & Lu, H. A survey on design, actuation, modeling, and control of continuum robot. *Cyborg and Bionic Systems* (2022).
- Liu, P., Din, A., Huang, L. & Yusuf, A. Stochastic optimal control analysis for the hepatitis B epidemic model. *Results Phys.* **26**, 104372 (2021).
- Biswas, M. H. A. Optimal control of Nipah virus (NiV) infections: A Bangladesh scenario. *J. Pure Appl. Math. Adv. Appl.* **12**(1), 77–104 (2014).
- Mondal, M. K., Hanif, M. & Biswas, M. H. A. A mathematical analysis for controlling the spread of Nipah virus infection. *Int. J. Simul. Model.* **37**(3), 185–197 (2017).
- Shah, N. H., Suthar, A. H., Thakkar, F. A. & Satia, M. H. SEI model for transmission of Nipah virus. *JMCS* **8**(6), 714–730 (2018).
- Nita, H. S., Niketa, D. T., Foram, A. T. & Moksha, H. S. Control strategies for Nipah virus. *Int. J. Appl. Eng.* **13**(21), 15149–15163 (2018).
- Agarwal, P. & Singh, R. Modelling of transmission dynamics of Nipah virus (Niv): A fractional order approach. *Physica A* **547**, 124243 (2020).
- Ullah, S., Nawaz, R., AlQahtani, S. A., Li, S. & Hassan, A. M. A mathematical study unfolding the transmission and control of deadly Nipah virus infection under optimized preventive measures: New insights using fractional calculus. *Results Phys.* **51**, 106629 (2023).
- Barua, S. & Dénes, A. Global dynamics of a compartmental model to assess the effect of transmission from deceased. *Math. Biosci.* **364**, 109059 (2023).
- Barua, S. & Dénes, A. Global dynamics of a compartmental model for the spread of Nipah virus. *Heliyon* **9**(9) (2023)
- Li, S., Ullah, S., AlQahtani, S. A. & Asamoah, J. K. K. Examining dynamics of emerging nipah viral infection with direct and indirect transmission patterns: A simulation-based analysis via fractional and fractal-fractional derivatives. *J. Math.* (2023).
- Van den Driessche, P. & Watmough, J. Reproduction numbers and sub-threshold endemic equilibria for compartmental models of disease transmission. *Math. Biosci.* **180**(1–2), 29–48 (2002).
- Chong, H. T., Jahangir Hossain, M. & Tan, C. T. Differences in epidemiologic and clinical features of nipah virus encephalitis between the Malaysian and Bangladesh outbreaks. *Neurology Asia*, pp. 23–26 (2008).

31. Sharma, Vikrant, Kaushik, Sulochana, Kumar, Ramesh, Yadav, Jaya Parkash & Kaushik, Samander. Emerging trends of nipah virus: A review. *Rev. Med. Virol.* **29**(1), e2010 (2019).
32. Bangladesh Population. <https://www.worldometers.info/worldpopulation/bangladesh-population/>
33. Rahman, Mahmudur & Chakraborty, Apurba. Nipah virus outbreaks in Bangladesh: A deadly infectious disease. *WHO South-East Asia J. Public Health* **1**(2), 208–212 (2012).
34. Mondal, M. K., Hanif, M. & Biswas, M. H. A. A mathematical analysis for controlling the spread of nipah virus infection. *Int. J. Model. Simul.* **37**(3), 185–197 (2017).
35. Khan, M. A., Ullah, S. & Kumar, S. A robust study on 2019-nCoV outbreaks through non-singular derivative. *Eur. Phys. J. Plus* **136**, 1–20 (2021).
36. Bangladesh population. <https://www.worldometers.info/world-population/bangladesh-population>. Accessed: March 2023.
37. Sinha, D. & Sinha, A. Mathematical model of zoonotic nipah virus in south-east Asia region. *ASMI* **2**(9), 82–89 (2019).
38. Zewdie, A. D. & Gakkhar, S. A mathematical model for Nipah virus infection. *J. Appl. Math.* **2020**, 1–10 (2020).
39. Zewdie, A. D., Gakkhar, S. & Gupta, S. K. Human-animal nipah virus transmission: Model analysis and optimal control. *Int. J. Dyn. Control* **11**(4), 1974–1994 (2022).
40. Chitnis, N., Hyman, J. M. & Cushing, J. M. Determining important parameters in the spread of malaria through the sensitivity analysis of a mathematical model. *Bull. Math. Biol.* **70**, 1272–1296 (2008).
41. Ullah, S. & Khan, M. A. Modeling the impact of non-pharmaceutical interventions on the dynamics of novel coronavirus with optimal control analysis with a case study. *Chaos Solit. Fractals* **139**, 110075 (2020).
42. Pontryagin, L. S., Boltyanskii, V. T., Gamkrelidze, R. V., Mishcheuko, E. F. & Works IV, L. P. S. *The Mathematical Theory of Optimal Processes*, *Class. Sov. Math.* (Gordon and Breach Science Publishers, 1986).
43. Chazuka, Z., Madubueze, C. E. & Mathebula, D. Modelling and analysis of an HIV model with control strategies and cost-effectiveness. *Results Control Optim.* **14**, 100355 (2024).
44. Ngina, P., Mbogo, R. W. & Luboobi, L. S. HIV drug resistance: Insights from mathematical modelling. *Appl. Math. Model.* **75**, 141–61 (2019).
45. Lukes, D. L. *Differential Equations: Classical to Controlled*. *Mathematics in Science and Engineering* Vol. 162 (Academic Press, 1982).
46. Augusto, F. B. & Leite, M. C. A. Optimal control and cost-effective analysis of the 2017 meningitis outbreak in Nigeria. *Infect. Dis. Model.* **4**, 161–187 (2019).

Acknowledgements

The authors extend their appreciation to the Deanship of Research and Graduate Studies at King Khalid University for funding this work through a Large Research Project under grant number RGP2/223/45.

Author contributions

M.Y.K. and S.U. conceptualized the main problem, wrote the original manuscript, and performed theoretical and simulation results. M.F. reviewed the entire mathematical results and Wrote the manuscript. A.B.S. performed basic mathematical results, validate all the results with care, and formal analysis. B.A.A. reviewed and restructured the manuscript, and funding acquisition. All authors are agreed on the final draft of the submission file.

Competing interests

The authors declare no competing interests.

Additional information

Correspondence and requests for materials should be addressed to A.B.S.

Reprints and permissions information is available at www.nature.com/reprints.

Publisher's note Springer Nature remains neutral with regard to jurisdictional claims in published maps and institutional affiliations.



Open Access This article is licensed under a Creative Commons Attribution-NonCommercial-NoDerivatives 4.0 International License, which permits any non-commercial use, sharing, distribution and reproduction in any medium or format, as long as you give appropriate credit to the original author(s) and the source, provide a link to the Creative Commons licence, and indicate if you modified the licensed material. You do not have permission under this licence to share adapted material derived from this article or parts of it. The images or other third party material in this article are included in the article's Creative Commons licence, unless indicated otherwise in a credit line to the material. If material is not included in the article's Creative Commons licence and your intended use is not permitted by statutory regulation or exceeds the permitted use, you will need to obtain permission directly from the copyright holder. To view a copy of this licence, visit <http://creativecommons.org/licenses/by-nc-nd/4.0/>.

© The Author(s) 2024